

## High-Resolution Study of $\text{Co}^{56}$ by $(d, \alpha)$ and $(\text{He}^3, p)$ Reactions\*

M. J. Schneider† and W. W. Daehnick

*Nuclear Physics Laboratory, University of Pittsburgh, Pittsburgh, Pennsylvania 15213*

(Received 4 June 1971)

Levels of  $\text{Co}^{56}$  up to 4.4-MeV excitation have been studied by the direct  $\text{Ni}^{58}(d, \alpha)\text{Co}^{56}$  reaction at a deuteron energy of 17 MeV. Experimental resolution of 9 to 12 keV permitted investigation of many previously unknown states.  $\text{Fe}^{54}(\text{He}^3, p)\text{Co}^{56}$  spectra at  $E_{\text{He}^3} = 18$  MeV were taken in order to supplement an earlier low-resolution study at the same energy. The total experimental resolution obtained for this reaction was 16 keV and permitted investigation of previously unresolved doublets. Accurate ( $\pm 0.3\%$ ) excitation energies were obtained for about 80  $\text{Co}^{56}$  levels.  $\text{Ni}^{58}(d, \alpha)\text{Co}^{56}$  angular distributions obtained by other investigators with 12- and 15-MeV deuterons had presented serious difficulties in the attempted analysis with distorted-wave Born-approximation (DWBA) calculations. At 17 MeV, given  $L$  values led to characteristic shapes which could be recognized empirically and crudely fit by "conventional" DWBA curves. Stock *et al.* had shown in 1967 that finite-range corrections become less important and DWBA results more reliable for  $(\text{He}^3, \alpha)$  if  $V_{\text{He}^3} + V_n \approx V_\alpha$ . We generalized this prescription to two-nucleon transfers and found similarly positive results, provided that the radii of all real wells were kept near  $1.2A^{1/3}$  fm. With this "well-matching" prescription our microscopic DWBA calculations were improved to the point that the correlation of  $L = 0, 2, 4, 6$  curves to positive-parity states became unambiguous. In the study of individual  $\text{Co}^{56}$  states we used  $(p, \text{He}^3)$  and  $(\text{He}^3, t)$  results of other investigators together with our own data to suggest  $J^\pi$  assignments or narrow  $J^\pi$  limits for 46 states. It was found particularly useful to investigate the  $\sigma(d, \alpha)/\sigma(p, \text{He}^3)$  ratio for given  $L$  transfer. As expected on theoretical grounds, cross sections for  $J^+$  (odd) levels showed large and nearly constant ratios. Ratios for transition strengths to known  $J^+$  (even) states were significantly smaller and vanished for  $T_>$  states. The properties of 15 low-lying levels could be correlated with those of states predicted in recent shell-model calculations by J. McGrory. The importance of two-particle-two-hole configurations in most of these states was demonstrated. Remaining discrepancies might be explained by a sizable four-hole-two-particle strength in  $\text{Ni}^{58}(\text{g.s.})$ .

### I. INTRODUCTION

From the shell-model point of view the spectrum of  $\text{Co}^{56}$  should be a fruitful object of study; for in the simplest analysis  $\text{Co}^{56}$  is just one proton hole and one neutron removed from the doubly magic nucleus  ${}_{28}\text{Ni}_{28}^{56}$ . Ideally, spectroscopy of  $\text{Co}^{56}$  ought to yield direct information on the particle-hole residual interaction in the  $f$ - $p$  shell.<sup>1,2</sup> If, on the other hand, the particle-hole description is too restrictive, comparison with calculations that consider two-particle-two-hole admixtures<sup>3</sup> as well ought to reveal whether this refinement is sufficient or, at least, constitutes a considerable improvement over the simpler model. Previously, theoretical calculations and experimental spectroscopic analyses have tried to describe  $\text{Co}^{56}$  in simple shell-model schemes, representing low-lying levels by pure or nearly pure shell-model configurations.<sup>1,2</sup> Lately, some experimental results<sup>4</sup> have led to consideration of configuration mixing in the  $\text{Co}^{56}$  wave functions.<sup>5</sup> Data in the present work lead to the conclusion that configuration mixing is even more extensive than has been previously recognized. Similarly, recent shell-model calculations of McGrory<sup>3</sup> predict extensive configura-

tion mixing in  $\text{Co}^{56}$ . Our data will be compared with these predictions and the earlier, more restricted calculations of Vervier.<sup>2</sup>

$\text{Co}^{56}$  is a difficult nucleus to reach experimentally. It cannot be formed by one-particle stripping or pickup reactions.  $\text{Fe}^{56}(p, n)\text{Co}^{56}$  experiments are possible, but impeded by the well-known difficulties of neutron spectroscopy. Hence, the earlier studies of  $\text{Co}^{56}$  consisted primarily of analyses of  $\gamma$  decay of the 1.718 level of  $\text{Co}^{56}$ , the product of electron capture<sup>6-9</sup> in  $\text{Ni}^{56}$ , and the two-nucleon-transfer reactions  $(\text{He}^3, p)$ <sup>4, 10, 11</sup> and  $(d, \alpha)$ .<sup>4, 10, 12, 13</sup> More recently  $\text{Co}^{56}$  has been investigated by  $(\text{He}^3, t)$ <sup>14-16</sup> and  $(p, \text{He}^3)$ <sup>17</sup> reactions. Theoretical studies, based to a greater or lesser degree on experimental results, have also been made by several groups.<sup>1-3, 5, 18</sup> Previous particle-transfer work has been hampered by modest resolution or low beam energy, the latter permitting sizable nondirect contributions. The drawback of previous  $\gamma$ -ray work is that it gives no information on states above the 1.718-MeV level.

In this work,  $\text{Co}^{56}$  levels up to 4.4 MeV in excitation are investigated with  $(d, \alpha)$  angular distributions at 17-MeV deuteron energy for  $7^\circ \leq \theta \leq 80^\circ$ . The experiment was prompted by

recent successes of the  $(d, \alpha)$  reaction as a spectroscopic tool in the  $f$ - $p$ <sup>19,20</sup> and higher<sup>21</sup> shells.

## II. EXPERIMENT

### A. General Comments

For this experiment, the Pittsburgh three-stage Van de Graaff was used in combination with the Enge split-pole spectrograph.<sup>22</sup> Thin targets and careful control of energy-broadening and back-ground-producing effects allowed typical experimental resolutions of 9–12 keV with peak-to-back-ground ratios of better than 1000 to 1. Close to 80 levels were observed and several previously unknown doublets were resolved. Reliable angular distributions were extracted for about 50 levels. At 17 MeV the  $\text{Ni}^{58}(d, \alpha)$  reaction proceeds primarily by the direct-transfer mechanism (i.e., it can be viewed as a one-step pickup process with no disturbance of the “core”) so data were taken with the expectation that they would be amenable to analysis by direct-transfer theories.<sup>23,24</sup> As part of the experiment several  $\text{Fe}^{54}(\text{He}^3, p)\text{Co}^{56}$  spectra were taken at 18 MeV, and for better dispersion along the focal plane and a better separation of multiplets, a  $(d, \alpha)$  spectrum was taken at 12 MeV.

### B. $\text{Ni}^{58}(d, \alpha)\text{Co}^{56}$

Films of typically  $35\text{-}\mu\text{g}/\text{cm}^2$  thickness were prepared by electron-gun evaporation of 99.89% pure  $\text{Ni}^{58}$  from a carbon crucible onto  $10\text{-}\mu\text{g}/\text{cm}^2$  carbon foils. The foils were floated onto target frames 1 in. high by 1.5 in. wide. Targets were checked for uniformity by bombardment with a 10-MeV  $\alpha$  beam and inspection of the elastic peak shape and half-width measured with a position-sensitive detector mounted in the spectrograph focal plane. Target thickness and lack of contamination were checked by exposure to an 11.8-MeV deuteron beam. The target thickness was calculated from the elastic counts at several angles and cross-section measurements in the literature<sup>25</sup> and was confirmed to within 6% by Rutherford scattering of 7-MeV  $\alpha$  particles in our 18-in. scattering chamber. High-resolution elastic deuteron scattering spectra showed no peaks greater than 0.4% of the  $\text{Ni}^{58}$  peak height, except for those from oxygen and unimportant lighter elements. For runs at angles below  $20^\circ$ , “line” targets were made<sup>26</sup> by evaporating  $\text{Ni}^{58}$  onto carbon foils through a mask with a 2-by  $\frac{1}{2}$ -mm hole. Line target data runs were normalized to “area” target runs at several overlapping angles.

Deuteron beam energy spread at 17 MeV was  $\sim 2$  keV. Typical beam current on the target was  $0.6$   $\mu\text{A}$ . A quadrupole lens positioned 106 cm before

the target focused the beam through a defining slit  $\frac{1}{2}$  mm wide and 2 mm high onto the target, 2 cm beyond the slit. The defining slit was followed by an antiscattering slit to obstruct slit scattered particles. A restricted width of the entrance aperture of the quadrupole lens controlled the beam divergence at the target, which was kept to  $0.8^\circ$  at small angles and  $0.5^\circ$  at large angles, where it gave the largest contribution to peak broadening. The angular acceptance of the spectrograph was  $\Delta\theta = 2.6^\circ$  and the solid angle subtended at the target by the spectrograph aperture was 1.4 msr. Reaction  $\alpha$  particles were detected by an array of four position-sensitive detectors<sup>26</sup> in the focal plane, all having apertures 8 mm high and 50 mm long. Peaks that fell into the 10-mm gaps between detectors were seen in duplicate runs taken at each angle with a small change in spectrograph magnetic field strength. More extensive discussions of the experimental setup and resolution contributions have been given elsewhere.<sup>26,27</sup>

Single-channel analyzers viewed the amplified energy signals ( $E$ ) from each position-sensitive detector and rejected the accompanying position  $x$  energy ( $XE$ ) signal unless the event was due to an  $\alpha$  particle. Inelastic deuterons were the principal source of rejected signals. Use of “line” targets was necessary at low angles in order to minimize slit scattering of the incident beam by wider beam collimating slits. Thus, for  $\theta \leq 20^\circ$ , the  $\frac{1}{2}$ - by 2-mm beam defining slit was replaced by a 3-mm circular slit, 5.5 cm upstream from the target, and the area (standard) target was replaced by a “line” target. Before each line target run the beam was tuned through the mask used in making the target, which was also mounted on the target ladder, in order to maximize the amount of beam hitting the target material during the run. For line targets charge normalization is of little value, since an unknown fraction of the beam passes through the Ni target material. In fact, charge normalization with very thin targets is in general less trustworthy than would be desirable, so all runs were normalized to the number of elastic counts in two NaI scintillation monitor detectors located at  $\pm 38^\circ$  in the scattering chamber, each subtending a solid angle of 0.164 msr. Disagreement between charge and monitor counter normalization was generally less than 6%. Typically 5000  $\mu\text{C}$  of charge were collected for each run at the larger angles and 2000  $\mu\text{C}$  at smaller angles. A typical  $\text{Ni}^{58}(d, \alpha)$  counter spectrum is shown in Fig. 1. 17-MeV runs with  $\alpha$ -sensitive photographic plates (50- $\mu$  Ilford K-1) in the focal plane were taken at  $30$  and  $50^\circ$  in order to check excitation-energy assignments and the reliability of the discrimination circuitry used with the position-sensi-

tive detectors. Agreement between emulsion and detector data was within the expected experimental error for the large majority of peaks.

The  $(d, \alpha)$  spectrum for  $\text{Co}^{56}$  shows well-separated states below and rather tightly packed states above 4 MeV. Average level strengths slowly decrease as excitation increases, but strong levels are seen throughout the spectrum. Excitation energies are given in Table I for all states that could be resolved, i.e., all well-separated states plus those states that stood out above the "continua" in either or both of the  $(d, \alpha)$  and  $(\text{He}^3, p)$  reactions. About 50 of these were strong, well-separated, and low enough in excitation to be resolved by the four position-sensitive detectors at all angles.

#### C. $\text{Fe}^{54}(\text{He}^3, p)\text{Co}^{56}$

$\text{Fe}^{54}$  of 97.1% purity was evaporated onto  $10\text{-}\mu\text{g}/\text{cm}^2$  carbon foils and targets were tested for uniformity, purity, and thickness as described above.  $(\text{He}^3, p)$  plate spectra were taken in the spectrograph at 15 and  $30^\circ$  with the 18-MeV  $\text{He}^3$  beam and with an average experimental resolution of  $\sim 16$  keV. These two angles were chosen for the possibility of getting an indication of  $L$  values for weaker peaks not seen or unresolved by Laget and Gastebois in their  $(\text{He}^3, p)$  experiment,<sup>4</sup> since their data indicate that the ratio  $\sigma(15^\circ)/\sigma(30^\circ)$  is quite different for  $L=2$  and 4 ( $\sim 2$  and  $\sim 0.6$ , respectively). The  $30^\circ$   $(\text{He}^3, p)$  spectrum is shown in Fig. 2.

#### D. Excitation-Energy Determination

Accurate ( $\pm 0.3\%$ ) excitation energies were obtained by comparison of  $\text{Co}^{56}$  and well-known spectra taken consecutively on the same nuclear emulsion plate. The code SPIRO<sup>28</sup> uses a known spectrum to calibrate the spectrograph for an accompanying unknown spectrum taken under the same conditions and gives excitation energies for the latter. Two calibration spectra were used:  $\text{Ni}^{61}$  and  $\text{Co}^{60}$ . Both are well known over several MeV from spectroscopy of cascade  $\gamma$  rays with  $\text{Ge}(\text{Li})$  detectors.<sup>29,30</sup>  $\text{Cu}^{63}(d, \alpha)\text{Ni}^{61}$  and  $\text{Ni}^{58}(d, \alpha)\text{Co}^{56}$  comparison spectra were taken at 12 and 17 MeV, and  $\text{Fe}^{54}(\text{He}^3, p)\text{Co}^{56}$  and  $\text{Co}^{59}(\text{He}^3, p)\text{Ni}^{61}$  spectra were taken at 18 MeV. The  $(d, \alpha)$  spectrum pairs agreed among themselves within 0.15% for the excitation energies of most peaks, but  $(\text{He}^3, p)$  excitation energies were systematically  $\sim 0.3\%$  higher than those obtained from  $(d, \alpha)$ . Having no reason to prefer one set over the other, we assigned to all peaks excitation energies halfway between the  $(d, \alpha)$  and  $(\text{He}^3, p)$  results, with an estimated scale error of  $< \pm 0.3\%$  of excitation energy. Differences between excited levels are uncertain to 2 keV or 0.3% of the energy difference, whichever is larger.

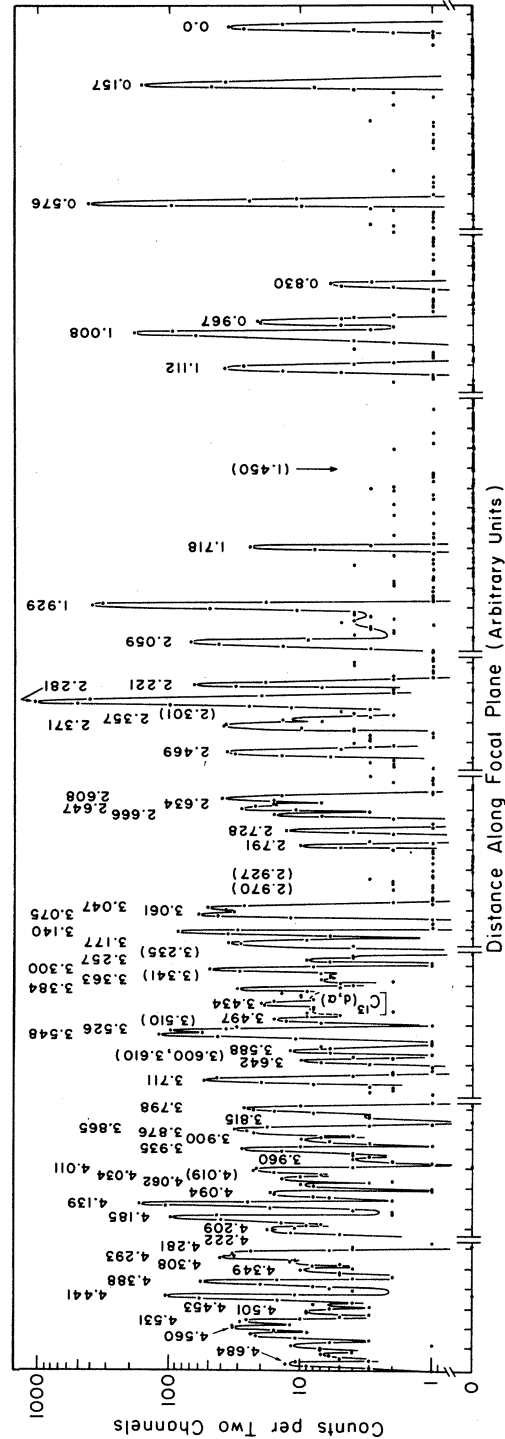


FIG. 1.  $\alpha$ -particle spectrum from the reaction  $\text{Ni}^{58}(d, \alpha)\text{Co}^{56}$  at  $E_d = 17$  MeV,  $\theta_{\text{lab}} = 35^\circ$ . This spectrum is a composite of two overlapping runs, each taken with four position-sensitive detectors, at slightly different spectrograph magnetic fields to cover the gaps between detectors. Compression of the energy scale by summation of pairs of adjacent channels degrades apparent resolution slightly.

TABLE I. Comparison of results of the present experiment with those of previous workers. Experiments prior to 1969 are summarized by the  $L$  values, excitation energies, and  $J^\pi$  adopted by M. N. Rao, Nucl. Data B3(Nos. 3, 4), 43 (1970). Also included are (He<sup>3</sup>,  $t$ ) results of Roos and Goodman (Ref. 14), ( $p$ , He<sup>3</sup>) excitations and  $L$  and  $J^\pi$  values of Bruge and Leonard (Ref. 17). For the present experiment, excitation energies, maximum ( $d$ ,  $\alpha$ ) cross sections (30° cross sections for the levels above 4.45 MeV),  $L(d, \alpha)$  values,  $L(\text{He}^3, p)$  values from the 15–30° cross-section ratio as explained in the text,  $J^\pi$  limits, and our best estimate of  $J^\pi$  are shown. Equivalence of higher levels seen in different reactions is not always certain.

Previous work										Present work				
Nuclear Data Sheets <sup>a</sup> (1970) adopted levels										(p, He <sup>3</sup> ) <sup>b</sup>				
$E_x$	$J^\pi$	$L(d, \alpha)$	$L(\text{He}^3, p)$	$E_x$	(He <sup>3</sup> , $t$ ) <sup>c</sup> $E_x$	$E_x$	$L$	$J^\pi$	$E_x$	$\sigma_{\text{max}}(d, \alpha)$ ( $\mu\text{b}/\text{sr}$ )	$L(d, \alpha)$	$L(\text{He}^3, p)$	$J^\pi$ limits	Best $J^\pi$
0.0	4 <sup>+</sup>	4?	...	0.0	0.0	0.0	4	4 <sup>+</sup>	0.0	16	4	...	(3 <sup>+</sup> ), 4 <sup>+</sup> , 5 <sup>+</sup>	4 <sup>+</sup>
0.1583	3 <sup>+</sup>	2	2	0.153	0.166	0.166	2+4	3 <sup>+</sup>	0.157	86	2	...	(1 <sup>+</sup> ), 2 <sup>+</sup> , 3 <sup>+</sup>	3 <sup>+</sup>
0.577	...	4	4	0.574	0.578	0.578	4+6	5 <sup>+</sup>	0.576	230	4	...	(3 <sup>+</sup> ), 4 <sup>+</sup> , 5 <sup>+</sup>	(5 <sup>+</sup> )
0.829	...	4?2?	...	0.831	0.840	0.840	4	4 <sup>+</sup> , 5 <sup>+</sup>	0.830	3.7	(4)	...	(3 <sup>+</sup> ), 4 <sup>+</sup> , 5 <sup>+</sup>	(4 <sup>+</sup> )
0.9705	2 <sup>+</sup>	...	2	0.974	0.961	0.961	2+4	3 <sup>+</sup>	0.967	12	2	(2)	(1 <sup>+</sup> ), 2 <sup>+</sup> , 3 <sup>+</sup>	2 <sup>+</sup>
1.008	...	4	...	...	1.001	1.001	2	2 <sup>+</sup>	1.008	100	4	(4)	(3 <sup>+</sup> ), 4 <sup>+</sup> , 5 <sup>+</sup>	(5 <sup>+</sup> )
1.113	...	2	...	...	1.106	1.106	4	4 <sup>+</sup> , 5 <sup>+</sup>	1.112	18	(2+4)	(2)	(1 <sup>+</sup> ), 2 <sup>+</sup> , 3 <sup>+</sup>	(3 <sup>+</sup> )
1.4512	(0) <sup>+</sup>	...	0	1.450	1.444	1.444	0	0 <sup>+</sup>	1.450 <sup>d</sup>	0	...	...	0 <sup>+</sup>	0 <sup>+</sup>
1.7209	1 <sup>+</sup>	0?	0+2	1.717	1.714	1.714	0+2	1 <sup>+</sup>	1.718	17	0	...	1 <sup>+</sup>	1 <sup>+</sup>
1.929	...	2	2	1.929	1.924	1.924	2+4	3 <sup>+</sup>	1.929	180	2	...	(1 <sup>+</sup> ), 2 <sup>+</sup> , 3 <sup>+</sup>	3 <sup>+</sup> (2 <sup>+</sup> )
2.058	...	2?	2	2.053	2.050	2.050	2	2 <sup>+</sup>	2.059	34	2	...	(1 <sup>+</sup> ), 2 <sup>+</sup> , 3 <sup>+</sup>	2 <sup>+</sup> (3 <sup>+</sup> )
2.224	...	...	...	(2.24)	2.220	2.220	2	2 <sup>+</sup>	2.221	32	2	(2)	(1 <sup>+</sup> ), 2 <sup>+</sup> , 3 <sup>+</sup>	3 <sup>+</sup> (2 <sup>+</sup> )
2.285 <sup>e</sup>	{	6	...	(2.30)	2.271	2.271	6	7 <sup>+</sup>	2.281	300	6	...	(5 <sup>+</sup> ), 7 <sup>+</sup>	7 <sup>+</sup>
2.359	{	...	2	...	...	...	...	...	2.301	<30	...	(2)	2 <sup>+</sup> , 3 <sup>+</sup>	(2 <sup>+</sup> , 3 <sup>+</sup> )
...	{	...	...	...	...	...	...	...	2.357	9	0	(2)	1 <sup>+</sup>	(1 <sup>+</sup> )
...	{	...	...	...	...	...	...	...	2.371	10	6	(2)	5 <sup>+</sup> , 6 <sup>+</sup> , 7 <sup>+</sup>	(6 <sup>+</sup> , 5 <sup>+</sup> , 7 <sup>+</sup> )
2.469	...	0?	4	...	2.456	2.456	0(+2?)	1 <sup>+</sup> ?	2.469	55	(4, 3)	(4)	...	...
2.608	...	...	...	...	...	...	...	...	2.608	23	2	(2)	(1 <sup>+</sup> ), 2 <sup>+</sup> , 3 <sup>+</sup>	(2 <sup>+</sup> , 3 <sup>+</sup> )
2.636	...	4	...	2.630	2.626	2.626	2	2 <sup>+</sup> , 3 <sup>+</sup>	2.634	36	(0)	(0)	(1 <sup>+</sup> )	(1 <sup>+</sup> )
...	...	...	...	...	...	...	...	...	2.647	15	(0)	...	(1 <sup>+</sup> )	(1 <sup>+</sup> )
2.667	...	...	...	2.705	{	{	...	...	2.666	8	(2)	...	(1 <sup>+</sup> ), 2 <sup>+</sup> , 3 <sup>+</sup>	(2 <sup>+</sup> , 3 <sup>+</sup> )
2.725	...	...	...	...	2.734	2.734	...	1 <sup>+</sup> ?	2.728	27	0	...	1 <sup>+</sup>	1 <sup>+</sup>
2.773	...	0?	...	...	...	...	...	...	2.791	2.5	...	...	...	...
2.926	...	...	2	2.950	2.946	2.946	...	...	{2.927	2.5	...	(2)	...	...
2.971	...	...	...	...	...	...	...	...	{2.970	4	(4)?	...	...	...
3.048	...	...	...	3.059	{	{	4	4 <sup>+</sup> ?	3.047	10	(5, 6)?	...	...	High
...	...	...	...	...	...	...	...	...	3.061	20	4	...	(3 <sup>+</sup> ), 4 <sup>+</sup> , 5 <sup>+</sup>	4 <sup>+</sup> (5 <sup>+</sup> )
3.073	...	...	2	...	...	...	...	...	3.075	25	2	...	(1 <sup>+</sup> ), 2 <sup>+</sup> , 3 <sup>+</sup>	2 <sup>+</sup> , 3 <sup>+</sup>

TABLE I (Continued)

Previous work				Present work								
Nuclear Data Sheets <sup>a</sup>				(p, He <sup>3</sup> ) <sup>b</sup>			(d, α)				Best J <sup>π</sup>	
(1970) adopted levels	(He <sup>3</sup> , t) <sup>c</sup>	E <sub>x</sub>	L (He <sup>3</sup> , p)	E <sub>x</sub>	L (proposed)	J <sup>π</sup> (proposed)	E <sub>x</sub>	σ <sub>max</sub> (d, α) (μb/st)	L (d, α)	L (He <sup>3</sup> , p)		J <sup>π</sup> limits
3.140 ...	...	...	...	3.137	2+4	3 <sup>+</sup> ?	9.140	77	2	...	(1 <sup>+</sup> ), 2 <sup>+</sup> , 3 <sup>+</sup>	3 <sup>+</sup> (2 <sup>+</sup> )
3.176 ...	3.162	...	2	{ ... }	...	...	3.177	18	(2)	...	...	...
3.244 e { ... }	...	...	...	{ ... }	...	...	3.235	3	(0)	...	(1 <sup>+</sup> )	(1 <sup>+</sup> )
3.295 ...	3.268	...	...	{ ... }	...	...	3.257	9	?	...	...	...
...	...	...	...	{ ... }	...	...	3.300	16	4	...	(3 <sup>+</sup> ), 4 <sup>+</sup> , 5 <sup>+</sup>	(4 <sup>+</sup> , 5 <sup>+</sup> )
...	...	...	...	...	...	...	3.341 <sup>d</sup>	...	...	...	...	...
3.379 ...	3.358	...	2	...	...	...	3.363	8	(3)?	...	...	...
...	3.412	...	...	{ 3.396 }	2	2 <sup>+</sup> , 3 <sup>+</sup>	3.384	8	?	...	...	...
3.431 ...	...	...	...	{ ... }	...	...	3.434	31	0	...	1 <sup>+</sup>	1 <sup>+</sup>
...	...	...	...	...	...	...	3.497	<5	...	...	...	...
3.505 e 0 <sup>+</sup> , 1 <sup>+</sup>	3.506	...	0	3.501	0	0 <sup>+</sup>	...	...	...	...	...	0 <sup>+</sup>
...	...	...	...	...	...	...	3.510	<5	...	...	...	...
...	...	...	...	...	...	...	3.526	17	(2)	...	...	...
...	...	...	...	...	...	...	3.548	30	6(+4)	...	5 <sup>+</sup> , 6 <sup>+</sup> , 7 <sup>+</sup>	...
3.577 (0) <sup>+</sup>	3.579	...	0	{ 3.587 }	0	0 <sup>+</sup>	...	...	...	...	...	(0 <sup>+</sup> )
3.587 ...	...	...	...	...	...	...	3.588	<5	...	...	...	...
...	...	...	...	...	...	...	3.600	10	...	...	...	...
...	...	...	...	...	...	...	3.610	2	...	...	...	...
...	...	...	...	...	...	...	3.642	7	(3)?	...	...	...
3.703 ...	3.680	...	...	...	...	...	3.711	40	(3)	...	...	...
3.796 ...	...	...	...	...	...	...	3.798	13	(6)	...	...	...
...	...	...	...	...	...	...	{ 3.815 }	8	(2)	...	(4)	...
3.846 ...	...	...	...	...	...	...	{ 3.865 }	20	(3, 4)	...	...	...
3.873 ...	...	...	...	...	...	...	3.876	10	(2)?	...	...	...
...	...	...	...	...	...	...	3.900	4	...	...	...	...
3.934 ...	...	...	...	...	...	...	3.935	9	...	...	...	...
...	...	...	...	...	...	...	3.960	...	...	...	(4)	...
4.062 ...	...	...	2	...	...	...	4.011	22	4	...	(3 <sup>+</sup> ), 4 <sup>+</sup> , 5 <sup>+</sup>	(4 <sup>+</sup> , 5 <sup>+</sup> )
...	...	...	...	...	...	...	4.019	...	...	...	...	...
...	...	...	...	...	...	...	4.034	10	(3)?	...	...	...
...	...	...	...	...	...	...	4.062	9	(3)?	(4)	...	...
...	...	...	...	...	...	...	4.094	7	?	...	...	...
...	...	...	...	...	...	...	4.139	95	4	...	(3 <sup>+</sup> ), 4 <sup>+</sup> , 5 <sup>+</sup>	(4 <sup>+</sup> , 5 <sup>+</sup> )
...	...	...	...	...	...	...	4.185	30	(2)?	...	...	...
...	...	...	...	...	...	...	4.209	<4	...	...	...	...
...	...	...	...	...	...	...	4.222	<4	...	...	...	...

TABLE I (Continued)

Previous work				Present work								
Nuclear Data Sheets <sup>a</sup> (1970) adopted levels				(p, He <sup>3</sup> ) <sup>b</sup>								
E <sub>x</sub>	J <sup>π</sup>	L(d, α)	L(He <sup>3</sup> , p)	(He <sup>3</sup> , t) <sup>c</sup>	L (proposed)	J <sup>π</sup>	E <sub>x</sub>	σ <sub>max</sub> (d, α) (μb/sr)	L(d, α)	L(He <sup>3</sup> , p)	J <sup>π</sup> limits	Best J <sup>π</sup>
				E <sub>x</sub>								
4.45	(2) <sup>+</sup>	...	2	...	2	2 <sup>+</sup>	4.432	...	2	...	(1 <sup>+</sup> ), 2 <sup>+</sup> , 3 <sup>+</sup>	(2 <sup>+</sup> , 3 <sup>+</sup> )
							...	...	...	...	...	...
							4.441	25	6(+4)	...	5 <sup>+</sup> , 6 <sup>+</sup> , 7 <sup>+</sup>	...
							4.281	11				
							4.293	~10				
							4.308	~10				
							4.349	<5				
							4.388	29				
							...	...				
							4.441	25	6(+4)	...	5 <sup>+</sup> , 6 <sup>+</sup> , 7 <sup>+</sup>	...
							4.453	σ(30°)				
							4.501	<10				
							4.531	<10				
							4.560	<10				
							4.684	<10				
							4.743	<10				
							4.768	16				
							4.846	~80				
							4.928	~80				
							4.991	~50				
4.993	...	...	...	...	...	...	...	...	...	...	...	...
5.097	...	...	...	...	2	3 <sup>+</sup>	5.090	~40	...	...	...	(3 <sup>+</sup> )
					2	2 <sup>+</sup>	5.187	~250	...	...	...	...
5.347							5.238	~80				
5.495												
8.92												

<sup>a</sup> M. N. Rao, Nucl. Data B3(Nos. 3, 4), 43 (1970).  
<sup>b</sup> Reference 17.

<sup>c</sup> Reference 14.  
<sup>d</sup> From (He<sup>3</sup>, p) spectra.

<sup>e</sup> Doublet.

Resultant excitation energies are in good agreement with the 1.721-, 1.451-, 0.971-, and 0.158-MeV level energies determined with a Ge(Li) detector by Piluso, Wells, and McDaniels.<sup>9</sup> Our present excitation energies are also well within the experimental errors of other particle-transfer experiments, although comparison becomes more difficult at high excitations due to poorer resolution in these earlier experiments and resultant inadvertent averaging over several states. A notable exception is the third strongest peak in the  $(d, \alpha)$  spectrum, which we see at  $5.146 \pm 0.015$  MeV. Bruge and Leonard<sup>17</sup> see this level as the strongest peak in the  $(p, \text{He}^3)$  spectrum at  $5.090 \pm 0.020$  MeV.

Sherr *et al.* are reported<sup>17</sup> to have seen a corresponding state at  $5.116 \pm 0.005$  MeV in  $(\text{He}^3, t)$ . Because of their size, there is little doubt that these peaks belong to the same level, but we have no explanation for the difference in observed energies.

### III. ANALYSIS OF THE $\text{Ni}^{58}(d, \alpha)$ REACTION

#### A. Expected Configurations

In the simplest shell-model picture of the  $0^+$  target nucleus  $\text{Ni}^{58}$  the  $1f_{7/2}$  proton and neutron shells are filled, and the two remaining neutrons occupy the  $2p_{3/2}$  orbital. Experiments<sup>31</sup> indicate, however, that the  $f_{7/2}$  neutron shell is 95% filled and the  $\geq 2$  remaining neutrons are distributed among the  $2p_{3/2}$ ,  $1f_{5/2}$ , and  $2p_{1/2}$  shells. Hence  $(d, \alpha)$  transfers to low-lying levels will most likely involve pickup of an  $f_{7/2}$  proton and an  $f_{7/2}$ ,  $p_{3/2}$ ,  $f_{5/2}$ , or  $p_{1/2}$  neutron. These configurations give a total of 20 simple positive-parity states, of which only 16 would be excited in this experiment, since  $(j)_{f=\text{even}}^2$  pickup is forbidden in  $(d, \alpha)$ .<sup>24</sup> The four remaining states involve transfer of an  $f_{7/2}$  proton and neutron coupled to  $J=0, 2, 4$ , or 6. If noticeable configuration mixing is present in these states, three of them should be seen through whatever components of their wave functions are *not* excited by  $(\pi f_{7/2}, \nu f_{7/2})$  pickup, but in any case  $0^+$  final states are still strongly forbidden. To the extent that the  $\text{Ni}^{58}$  ground state contains proton holes in the  $f_{7/2}$  shell it should also be possible to see states formed by coupling of  $p_{3/2}$  and higher protons to nearby neutron states, leading to many more levels than those mentioned above.

Negative-parity states in  $\text{Co}^{56}$  are expected only at higher excitations. They would be excited through transfer of a  $d_{3/2}$  proton or (less likely) a  $g_{9/2}$  neutron coupled to a neutron or proton from the  $1f$  or  $2p$  shells.

#### B. Distorted-Wave Born-Approximation Formalism

The zero-range distorted-wave Born-approximation (DWBA) calculation of the cross section

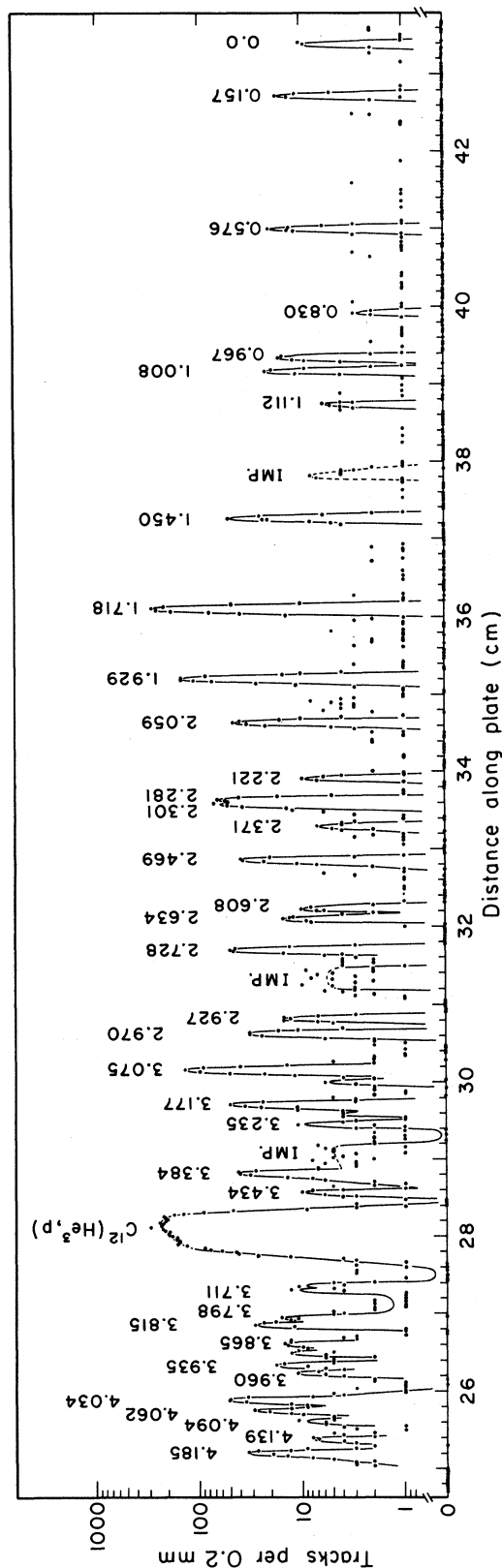


FIG. 2. Proton spectrum from the reaction  $\text{Fe}^{54}(\text{He}^3, p)\text{Co}^{56}$  at  $E_{\text{He}^3} = 1.8$  MeV and  $\theta_{\text{lab}} = 30^\circ$ . This spectrum was taken on a  $25\text{-}\mu$  Kodak NTB emulsion. Resolution is  $\sim 16$  keV.

for direct deuteron pickup yields an incoherent sum over  $L$ ,  $S$ ,  $J$ , and  $T$  which can be written<sup>24</sup>

$$\sigma(\theta) \propto N(1, 2) \sum_{SLJT} \left| \int [\psi_2^{(-)}(\vec{k}_2, \vec{R})]^* \tilde{U}_{LSJT}(R) \times Y_L^M(\hat{R}) \psi_1^{(+)}\left(\vec{k}_1, \frac{A-2}{A}\vec{R}\right) d\vec{R} \right|^2, \quad (1)$$

where  $S$ ,  $L$ ,  $J$ , and  $T$  are the spin, orbital angular momentum, total angular momentum, and isospin, respectively, of the transferred pair. Here particle 1 is the incoming deuteron, particle 2 is the outgoing  $\alpha$  particle,  $\vec{R}$  is the center-of-mass coordinate of the transferred  $p$ - $n$  pair,  $\psi_2^{(-)}$  and  $\psi_1^{(+)}$  are the outgoing and incoming scattered waves for the  $\alpha$  particle and deuteron.  $\tilde{U}_{LSJT}$  is the form factor, which plays a critical role in this theory, and  $Y_L^M$  are spherical harmonics. The over-all normalization  $N(1, 2)$  is dependent only on the type of reaction, here  $(d, \alpha)$ . There is some experimental evidence that within the framework of certain sets of calculations<sup>21, 32</sup>  $N(d, \alpha)$  is of the order of 40 (with an uncertainty of a factor of 2) so that some information can be extracted from comparison of calculated and experimental cross sections on an absolute scale.

### C. Two-Nucleon-Transfer Theory

The form factor in Eq. (1) can be written as

$$\tilde{U}_{LSJT} = \sum_{\gamma} \beta_{\gamma LSJT} f_{L\gamma}(R), \quad (2)$$

with

$$f_{L\gamma}(R) = \sum_N g_{NL\gamma} U_{NL\gamma}(R),$$

where  $\beta_{\gamma}$  is the "spectroscopic amplitude" for the configurations  $\gamma$ ;

$$\gamma = [\pi(nl j) \nu(n' l' j')].$$

$\beta_{\gamma}$  gives the overlap of the target nucleus with the final nucleus plus two nucleons in the configuration  $\gamma$ . The square of  $\beta_{\gamma}$  is analogous to the usual spectroscopic factor for one-particle-transfer reactions.  $U_{NL\gamma}$ , analogous to the single-particle-transfer case, is a term of the radial wave function for the c.m. of the transferred nucleons. The sum over  $N$  is necessary to adequately represent their c.m. motion. The factor  $g_{NL\gamma}$ , which weights the contributions of the various  $N$ , is written as a sum over terms of three overlap factors<sup>19, 24</sup>

$$g_{NL\gamma} = g \Omega_n \langle n\lambda, NL, L | n_{\pi} l_{\pi} n_{\nu} l_{\nu}; L \rangle, \quad (3)$$

where  $g$  is a symmetry factor here  $\equiv 1$ ,  $\langle \dots | \dots \rangle$  is the Moshinsky bracket which arises for the transformation from  $\vec{r}_{\pi}, \vec{r}_{\nu}$  to  $\vec{R}_{c.m.}, \vec{r}_{relative}$  coordinates in the calculation of the form factor, and  $\Omega_n$  is a measure of the overlap of the relative  $n$ - $p$  motion in the nucleus with their relative motion in

the  $\alpha$  particle.

Although the number of contributing  $L$  values for  $0^+$  targets is limited to one or two ( $L=J$  or  $L=J \pm 1$ ), there is no *a priori* limit on the number of configurations  $\gamma$  that can contribute to a given transition. The contributing configurations depend on the wave functions of the initial and final states and on any selection rules governing the transfer of a given  $p$ - $n$  pair. Under the usual direct-reaction assumptions,<sup>24</sup> there is a natural-parity requirement on  $(d, \alpha)$  transitions so that  $\pi_f = \pi_i (-1)^L$ . Furthermore, only  $S=1$  is allowed, so  $L = \text{even}$  can lead to  $J^{\pi} = (L-1, L, \text{ or } L+1)^+$ . A unique feature of two-nucleon-transfer reactions is that different configurations  $\gamma$  contribute coherently to the transition amplitude and so interference effects between them play an important role.

Moshinsky brackets are calculable exactly and have been tabulated<sup>33</sup> and thus are easy to insert into  $g_{NL\gamma}$ . Calculation of  $\Omega_n$  becomes simple if one assumes that the  $p$ - $n$  pair is in a relative  $s$  state.

For  $\beta_{\gamma}$  Glendenning gives the expression

$$\beta_{\gamma LSJ}(J_1, J_2) = \left( \frac{A+2}{2} \right)^{1/2} \int [\psi_{J_1}^*(\vec{A}) \phi_{\gamma LSJ}^*(\vec{r}_{\pi}, \vec{r}_{\nu})]_{J_2} \times \psi_{J_2}(\vec{A}, \vec{r}_{\pi}, \vec{r}_{\nu}) d\vec{A} d\vec{r}_{\pi} d\vec{r}_{\nu}, \quad (4)$$

where  $\binom{A+2}{2}$  is a symbolic multiplicity factor which for wave functions in the  $n$ - $p$  formalism and for the  $(d, \alpha)$  reaction is equal to  $\binom{N+1}{1} \binom{Z+1}{1} = (N+1)(Z+1) = n_{\nu} n_{\pi}$ , where  $n_{\nu}$  and  $n_{\pi}$  are the number of neutrons and protons, respectively, in the shells from which each is picked up.  $\psi_{J_1}$  is the wave function of the final nucleus,  $\phi_{\gamma LSJ}$  is the c.m. wave function of the two transferred nucleons in configuration  $\gamma$ ,  $\psi_{J_2}$  is the wave function of the target nucleus, and  $\vec{r}_{\pi}$  and  $\vec{r}_{\nu}$  are the position vectors of the two picked-up nucleons. (For Ni<sup>58</sup> we have  $J_2 \equiv 0$ .)  $\beta_{\gamma}$  is evaluated by separating  $\psi_{J_2}$  into proton and neutron wave functions and then recoupling into core plus transferred nucleons in  $L \cdot S$  coupling. (For the calculations of this study the amplitudes  $\beta_{\gamma LSJ}$  were available from the work of McGrory.<sup>3</sup>)

Considering the simplest Ni<sup>58</sup> configuration of closed  $f_{7/2}$  shells plus two neutrons, and the transfer of one of these valence neutrons plus an  $f_{7/2}$  proton, we obtain

$$\beta_{\gamma LSJ}(J, 0) = \left( \frac{n_{\pi} n_{\nu} (2J+1)}{(2j_{\pi}+1)(2j_{\nu}+1)} \right)^{1/2} \begin{bmatrix} l_{\pi} & \frac{1}{2} & j_{\pi} \\ l_{\nu} & \frac{1}{2} & j_{\nu} \\ L & S & J \end{bmatrix}, \quad (5)$$

where the square bracket is an  $LS$ - $JJ$  transformation coefficient. This result is easily derived from Glendenning's expression for two nucleons picked up from different shells.



The spectroscopic amplitudes for mixed-configuration wave functions can easily be found from that given above for pure configurations. If there are  $N$  terms (with coefficients  $C_i^{(1)}$ ) of the Ni<sup>58</sup> ground-state wave function that can each be matched with a term of the Co<sup>56</sup> wave function (with coefficient  $C_i^{(2)}$ ) such that each Co<sup>56</sup> term differs from the matching Ni<sup>58</sup> term only by the absence of a  $p$ - $n$  pair in configuration  $[l_\pi, l_\nu] = \gamma$ , then the spectroscopic amplitude for pickup of configuration  $\gamma$  leading to that Co<sup>56</sup> level is

$$\beta_{\gamma LSJ}(J, 0) = \sum_{i=1}^N C_i^{(1)} C_i^{(2)} \left( \frac{n_\nu^i n_\pi^i (2J+1)}{(2j_\pi+1)(2j_\nu+1)} \right)^{1/2} \begin{bmatrix} l_\pi & \frac{1}{2} & j_\pi \\ l_\nu & \frac{1}{2} & j_\nu \\ L & S & J \end{bmatrix}. \quad (6)$$

#### D. Inputs to the Distorted-Wave Calculations

##### 1. Microscopic Form Factor

Many angular distributions were obtained by distorted-wave calculations with code DWUCK<sup>34</sup> using external form-factor inputs. The form factors  $f_{L\gamma}$  were calculated by code MIFF of Drisko and Rybicki<sup>19,35</sup> from the Woods-Saxon (W-S) wave functions of the picked-up neutron and proton in several configurations in the  $1f$  and  $2p$  shells of Ni<sup>58</sup>. The single-nucleon wave functions were obtained as Woods-Saxon well eigenfunctions with well geometry<sup>36</sup> of  $r_0 = 1.17$  fm,  $r_c = 1.25$  fm, and  $a = 0.75$  fm. The nucleon separation energies determining the well depths were taken as half the sum of the  $n+p$  separation energies plus level excitation energy  $E^*$ . The asymptotic behavior of the total form factor  $\tilde{U}_L = \sum_\gamma \beta_\gamma f_{L\gamma}$  is determined by this separation energy, but since the effect on angular distributions is weak, calculations were done for  $E^* = 1$  and 3 MeV only. A mild dependence of calculated cross-section shapes on excitation energy was noted. For the single-nucleon wave functions a spin orbit strength 25 times the Thomas term was used. The size parameter for the  $\alpha$  particle was taken as  $\beta$  (MIFF) =  $9/8\langle r^2 \rangle = 0.43$  which corresponds to  $\eta = 0.23$  in Glendenning's notation.<sup>24</sup>

The code MIFF expands each W-S eigenfunction over principal quantum number  $n_i$  as a series of (10) harmonic-oscillator eigenfunctions, since the latter are more convenient to manipulate. The overlaps of W-S solutions and the harmonic-oscillator series were always extremely good out to the maximum radius used (15 fm). The neutron and proton expansions are then multiplied and a Talmi transformation<sup>37</sup> to relative and c.m. coordinates is made for each term of the product wave function. By integrating over the product of the two-nucleon relative motion in the target nu-

cleus and in the  $\alpha$  particle (assuming a Gaussian wave function for the latter)  $\Omega_n$  is calculated.

The code MIFF also has the capability of searching on W-S parameters for a bound "deuteron" well whose eigenfunction with the proper quantum numbers (the "cluster" form factor) comes closest to the microscopic form factor. In most of the calculations microscopic form factors were used, since the contributing microscopic terms  $f_{L\gamma}$  can be easily added in DWUCK, but for  $L=0$  a significant difference was observed between the microscopic and cluster form-factor shapes and slopes at and just outside the nuclear surface. This form-factor difference gave a phase difference between the two cross-section predictions – the cluster wave function, with a typical W-S slope, giving minima closer in towards  $0^\circ$  than the calculation using the microscopic form factor. The cluster predictions are in better agreement with the data.

##### 2. Optical-Model Well Parameters

In DWBA analyses of particle-transfer reactions<sup>19,21</sup> it is often sufficient to use optical parameters for the incoming and outgoing channels which are taken directly from the literature, after making sure, perhaps, that they are of the correct "family" (e.g., deuteron real well depths should have  $V_0 \sim 100$  MeV and radii  $r_0 \sim 1.1$  fm). In the course of this work detailed studies were made<sup>38</sup> of the effects of different combinations of published deuteron and  $\alpha$  potentials on the agreement of DWBA calculations with known experimental  $L=0, 2, 4, 6$  angular distributions. Various deuteron parameters of Perey and Perey<sup>39</sup> and  $\alpha$  parameters of McFadden and Satchler<sup>40</sup> and Bock<sup>41</sup> were used. It was found that each of the combinations tried yielded good predictions for some  $L$  values, but poor ones for others. The combination of a 98.6-MeV deuteron well and a 206.8-MeV  $\alpha$  well (with  $r_0 = 1.3$ ) appeared to be slightly superior to the others, but several fits remained unsatisfactory. Moreover, finite-range parameters corresponding to the Henley and Yu<sup>42</sup> choice of nucleon-nucleon interaction range = 0.63 fm (which gave the best fits) resulted in an enhancement of the surface contribution by a factor of 5, a correction so large as to cast serious doubts on the validity of the method.

The two-nucleon finite-range correction used<sup>43</sup> contains a dominant term  $\sim \exp[\text{const}(-V_i - V_{ff} + V_0 + S_{ff})]$ , where  $V_i$ ,  $V_{ff}$ , and  $V_0$  are the real well depths (as functions of  $R$ ) for the incoming particle, form factor, and outgoing particle, respectively, and  $S_{ff}$  is the binding energy of the transferred cluster. From examination of the parameters, it

is clear that the large surface enhancement results from the oversized  $\alpha$  well radius and depth. It seems, then, that limitations may be needed for the continuous ambiguities of the parameter sets. If, for example, the real well radii of the deuteron and  $\alpha$  particles were more nearly equal the calculated finite-range correction would be much smaller. Earlier Stock *et al.*<sup>44</sup> showed that for ( $\text{He}^3, \alpha$ ) calculations use of parameters satisfying

$$V_a + V_x \approx V_{a+x}, \quad (7)$$

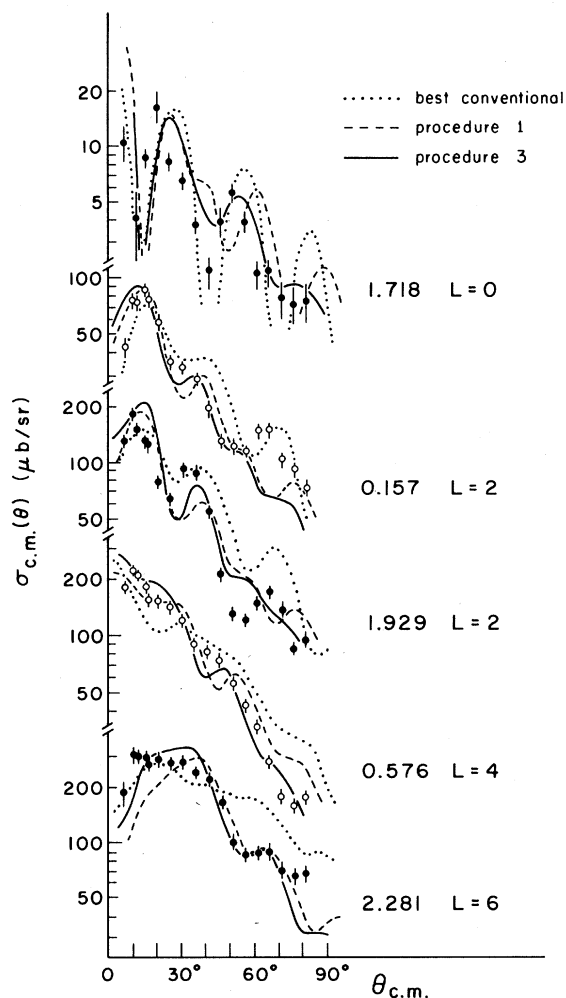


FIG. 3. Comparison of DWBA calculations for angular distributions of known  $L$  values using several sets of optical-model parameters. Dotted line: using deuteron and  $\alpha$  parameters directly from the literature (Refs. 39 and 40, respectively). Dashed line: using the same deuteron parameters, but changing the real well radius and diffusivity of the  $\alpha$  parameters to agree with the deuteron parameters (procedure 1). Solid line: refitting the  $\alpha$  elastic cross section and original deuteron scattering data requiring both  $r_0$  to be 1.2 and both diffusivities to be similar (procedure 3).

where  $a$  is the lighter projectile and  $x$  the transferred nucleon or cluster, not only minimizes the finite-range correction, but appears necessary for the reliability of the DWBA approximation itself. Similar considerations might apply for ( $d, \alpha$ ) calculations, so new sets of parameters were generated and the resulting DWBA predictions compared with experimental angular distributions. In the first test the  $\alpha$  real well radius and diffusivity in the 206.8-MeV parameter set were simply set equal to those of the deuteron real well. In a second test the  $\alpha$  elastic cross sections of Bock *et al.*<sup>41</sup> were refitted with the requirements  $r_0 = 1.109$ ,  $a = 0.709$ , and  $V_0 \sim 200$ . The fit was only fair but at least maintained good qualitative agreement with  $\alpha$  elastic scattering, which the first procedure did not. Finally the  $\alpha$  elastic cross sections and the original deuteron scattering data were *both* refitted with a fixed value  $r_0 = 1.2$ , while the diffusivities were allowed to vary in order to improve the fits.  $\langle \chi^2 \rangle$  for the deuteron fit went from the original value of 1.1 to 1.7, and  $\langle \chi^2 \rangle$  for the new  $\alpha$  parameters was 1.9, a fit almost as good as the original one. Results of procedures 1 and 3 are compared in Fig. 3 with the best previous calculations.

The conventional calculation does a poor job reproducing the  $L=6$  and  $L=4$  states shown. The  $L=0$  calculation is  $\sim 7^\circ$  out of phase with the data, as are the 1.929- and 0.157-MeV  $L=2$  curves. All three well-matching procedures led to better fits than could be achieved with the conventional approach. Procedure-1 calculations show decided improvement in the  $L=6$  calculation and in the  $L=2$  fits at 0.157 and 1.929, as well as in the 0.576 and 0.830  $L=4$  fits. It is remarkable that a drastic change in the  $\alpha$  geometry, guided solely by the requirement to agree with the deuteron geometry (procedure 1) would improve the fits so much. Procedure 3 leads to further improvements, but of a less striking nature. It seems that the "well-matching" criterion is at least as important in these ( $d, \alpha$ ) transfer calculations as a good overlap of the distorted waves used with those determined in scattering experiments.

The ( $d, \alpha$ ) reaction, like ( $\text{He}^3, \alpha$ ), has a considerable momentum mismatch for most  $L$  values, and therefore DWBA ( $d, \alpha$ ) calculations are expected to be less reliable than usual.<sup>45</sup> It has been pointed out<sup>4, 44</sup> that the momentum mismatch leads to dependence of the transition amplitude on  $\alpha$  partial waves not well determined in the optical-model fitting process. Our present studies emphasize the importance of criterion 7, which tends to prescribe the phase shifts for partial waves not well determined in elastic scattering by fixing  $r_0$  at 1.2 fm, a radius close to the nuclear radius as determined by electron and nucleon scattering experi-

ments.<sup>36</sup> The success of procedure 1 here and elsewhere<sup>43</sup> shows that the best elastic scattering parameters do not necessarily produce optimal fits in transfer reactions.

Procedures 2 and 3 give only small further improvements in agreement between data and calculations, which indicates that the introduction of the well-matching criterion is primarily responsible for the improved agreement. When procedure 3 is used  $L=0$  and 6 calculations are clearly improved, although the former is still somewhat out of phase with the data. It gives best fits to strong states with angular distributions typical for each  $L$  and hence is used in all further calculations of angular distributions.

For procedures 1, 2, and the conventional calculation, the use of microscopic form factors happened to give the best fits. However, for procedure 3 the cluster form factor (with  $r_0$  and  $a$  equal to those of the  $\alpha$  well, and  $V_0$  calculated by DWUCK from the deuteron binding energy) gave better fits. We have noticed this preference for cluster form factors previously, but have no physical explanation for it. Mathematically, the radial wave function for the "deuteron" generated in a given well tends to have a somewhat larger rms radius than the equivalent microscopic form factor, which is a product of single-particle wave functions generated in the well of the same geometry (typical values are  $r_0 = 1.2$  fm,  $a = 0.72$  fm). One might argue that the treatment of the transferred neutron-proton pair in the standard DWBA theory as noninteracting particles is too rough an approximation. On the other hand, the deuteron cluster model approach implying a 100%  $n$ - $p$  correlation appears even less realistic.

We conclude that the well-matching criterion 7 gives drastic improvements for calculated  $L=4$  and 6 angular distributions and slight improve-

ment for  $L=2$  and  $L=0$ . The optical parameters calculated by procedure 3, shown in Table II, give the best over-all fit to all four  $L$  values if cluster form factors, as described above, are used. The cluster approach is used below in all calculations of angular distributions for states of unknown configuration, but recourse is made to microscopic form factors for investigation of the configuration dependence of cross-section shapes, and the determination of predicted strengths for those transitions whose transfer amplitudes have been calculated by McGrory.

## E. Comparison with Data

### 1. Transfer Calculations

Recently McGrory calculated Ni<sup>58</sup> and Co<sup>56</sup> wave functions<sup>3</sup> along with transfer strengths for deuteron pickup. He used single-particle energies which are consistent with the Ni<sup>57</sup> spectrum and Kuo-Brown matrix elements for the effective two-body Hamiltonian. His calculation represents Co<sup>56</sup> as a Ca<sup>40</sup> core plus 14 or 15 nucleons in the  $f_{7/2}$  shell and the remainder in the  $p_{3/2}$ ,  $f_{5/2}$ , or  $p_{1/2}$  orbits, and Ni<sup>58</sup> wave functions as 16, 15, or 14  $f_{7/2}$  nucleons with the remaining 2, 3, or 4 nucleons again distributed among the three higher orbits. This is the largest space in which Co<sup>56</sup> shell-model calculations have been done to date, and contains considerably more Co<sup>56</sup> levels than the 19 simpler states mentioned earlier. McGrory computed Ni<sup>58</sup>-Co<sup>56</sup> two-nucleon spectroscopic amplitudes for 28 levels (four of each  $J^+$ ) below 4.3 MeV. For low excitations the predicted levels could be correlated to levels seen in the  $(d, \alpha)$  experiment. Differences in excitation energy were never more than a few hundred keV and often much smaller. McGrory's wave functions indicate extensive configuration mixing, a prediction which

TABLE II. Optical-model parameters used in DWUCK. The combination of lines 2 and 5, obtained by procedure 3 (see text), was used in all final calculations. All well depths are in MeV and distances in femtometers. The Bock parameters fit  $\alpha$  scattering from several nuclei in this mass region. The elastic  $\alpha$  cross section on Co<sup>56</sup> at 23.5 MeV calculated with Bock's parameters was used as "data" to get the parameters given in line 5.

Channel	Source	$V$ (MeV)	$r_0$ (fm)	$a$ (fm)	$r_c$ (fm)	$W_{vol}$ (MeV)	$4W_{surf}$ (MeV)	$r'_0$ (fm)	$a'$ (fm)	$\chi^2$
$d$ -Ni <sup>58</sup>	Perey and Perey, set b (Ref. 39)	98.6	1.105	0.709	1.105		65.96	1.17	0.831	1.1
$d$ -Ni <sup>58</sup>	Present work	88.5	1.2	0.629	1.105		65.98	1.11	0.860	1.7
$\alpha$ -Co <sup>58</sup>	McFadden and Satchler (Ref. 40)	206.8	1.41	0.519	1.3	25.8		1.41	0.519	1.62
$\alpha$ -Cr <sup>53</sup> to Ni <sup>60</sup>	Bock (Ref. 41)	183.7	1.4	0.564	1.3	26.6		1.4	0.564	
$\alpha$ -Co <sup>56</sup>	Present work	191.9	1.2	0.724	1.3	14.5		1.67	0.564	1.9

seems to be borne out by present data.

The predicted deuteron-transfer strengths were used to extract a value for the reaction normalization factor  $N(d, \alpha)$ . In contrast to some previous results using different calculational parameters<sup>21,32</sup> we find  $N(d, \alpha)$  close to 900. However, we must emphasize that this factor is strongly dependent on several details of the calculations (such as single-particle well sizes and  $\alpha$  size parameter in MIFF, optical-model parameters, and finite-range corrections in DWUCK), so that an unqualified comparison between the previous and present results is inappropriate. Our determination of  $N$  was made by comparison of predicted and measured cross sections for eight low-lying  $\text{Co}^{56}$  states, with par-

ticular consideration of the 2.281-MeV ( $\pi f_{7/2}^{-1}, \nu f_{7/2}^{-1}$ )<sub>7+</sub> level. (All nuclear configurations will be written with respect to a  $\text{Ni}^{58}$  vacuum.) Since the  $f_{7/2}$  shell is well filled in  $\text{Ni}^{58}$  and since there is only one  $(d, \alpha)$  transfer to a  $7^+$ ,  $T_c$  level, this level is the best place to determine  $N$ . The normalization factor for the 2.281-MeV level was  $N=1150$ , and for all eight levels considered, the result was  $N=890$ , with a standard deviation of 40%.

On the average, use of various combinations of optical-model parameters from the literature (all with wider  $\alpha$  wells) tended to give calculated cross sections higher by a factor of  $\sim 2$  than the matched well parameters used. Cross sections calculated

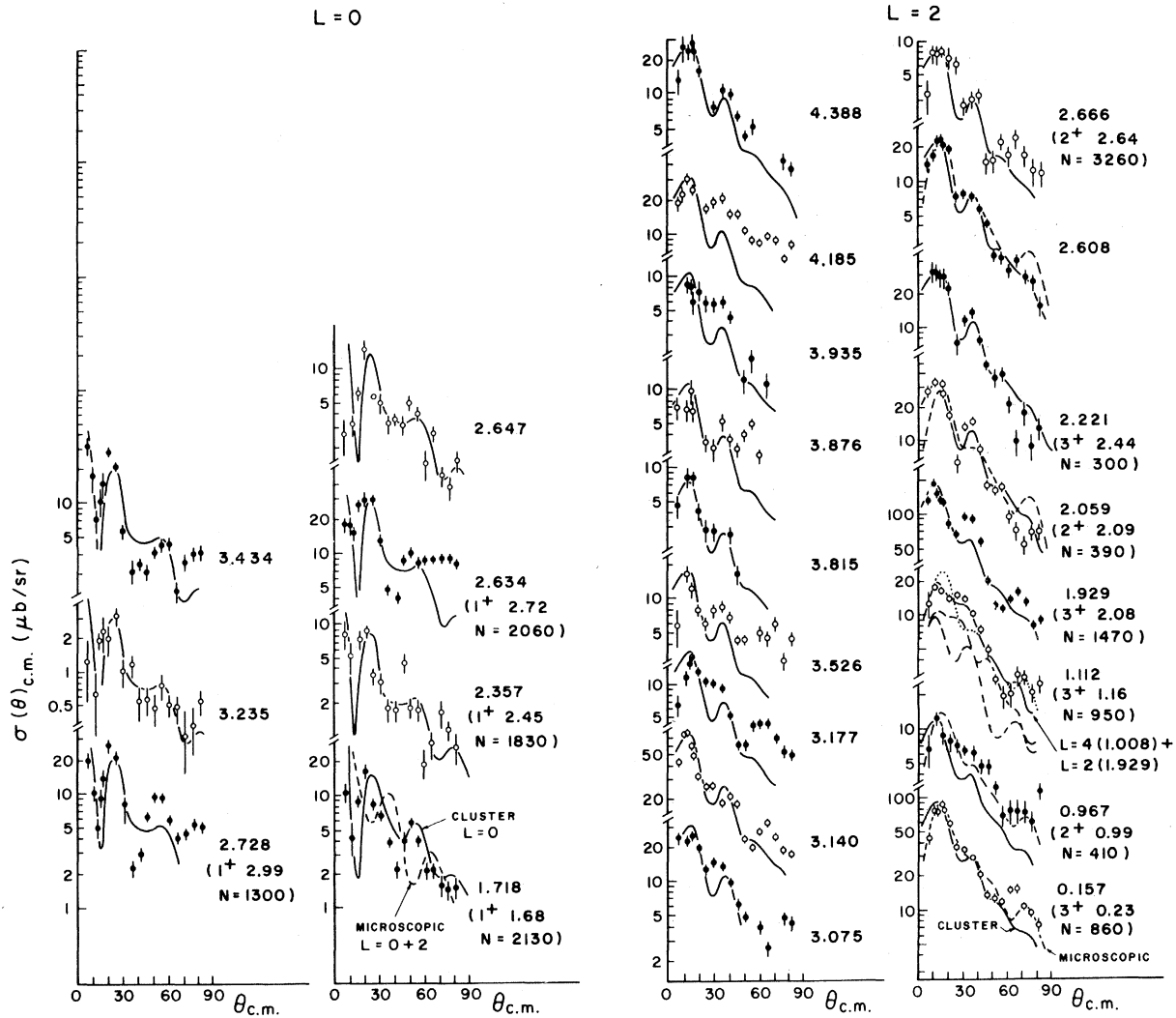


FIG. 4. Experimental  $(d, \alpha)$  cross sections and DWBA calculations for  $L=0$  and 2. The absolute scale error is about 15%. Error bars shown represent statistical, monitoring, background, and multiplet separation errors added in quadratures. Those states with  $J^\pi$  given after the excitation energy are identified with McGrory's predicted levels. The predicted excitation energies and normalizations  $N(d, \alpha)$  are also given.

without finite-range correction were roughly 30% higher; and calculations using, as far as possible, the form-factor parameters used in Ref. 21 produced cross sections larger by a factor of  $\sim 5$ . This indicates that a major source of disagreement between the present and previous normalization factors  $N$  is the mode of calculating the form factor. The combined effects of these differences in the calculations account for a factor of about 10. There is a remaining discrepancy of  $\sim 400/900$ , which is not understood at this time.

## 2. Experimental Angular Distributions

Figures 4 and 5 show angular distributions for 51 levels, grouped by  $L$  value. Those states with  $J^\pi$  indicated are identified with McGrory's predict-

ed states.  $L, J^\pi, \sigma_{\max}$ , and the excitation energies are also listed in Table I. Most angular distributions have one dominant  $L$ , in agreement with theoretical expectations.<sup>3</sup> In general, for those angular distributions not well fitted by a single  $L$ , addition of another allowed  $L' = L \pm 2$  would not improve the fit significantly.

Errors assigned to data points are due mainly to statistical and random monitoring errors, but for some levels background subtraction and multiplet separation uncertainties added to the estimated error. In cases where the same peak was measured repeatedly at the same angle, data points are the weighted means of all measurements. The absolute cross-section scale error (not indicated in the figure) arises primarily from imperfect

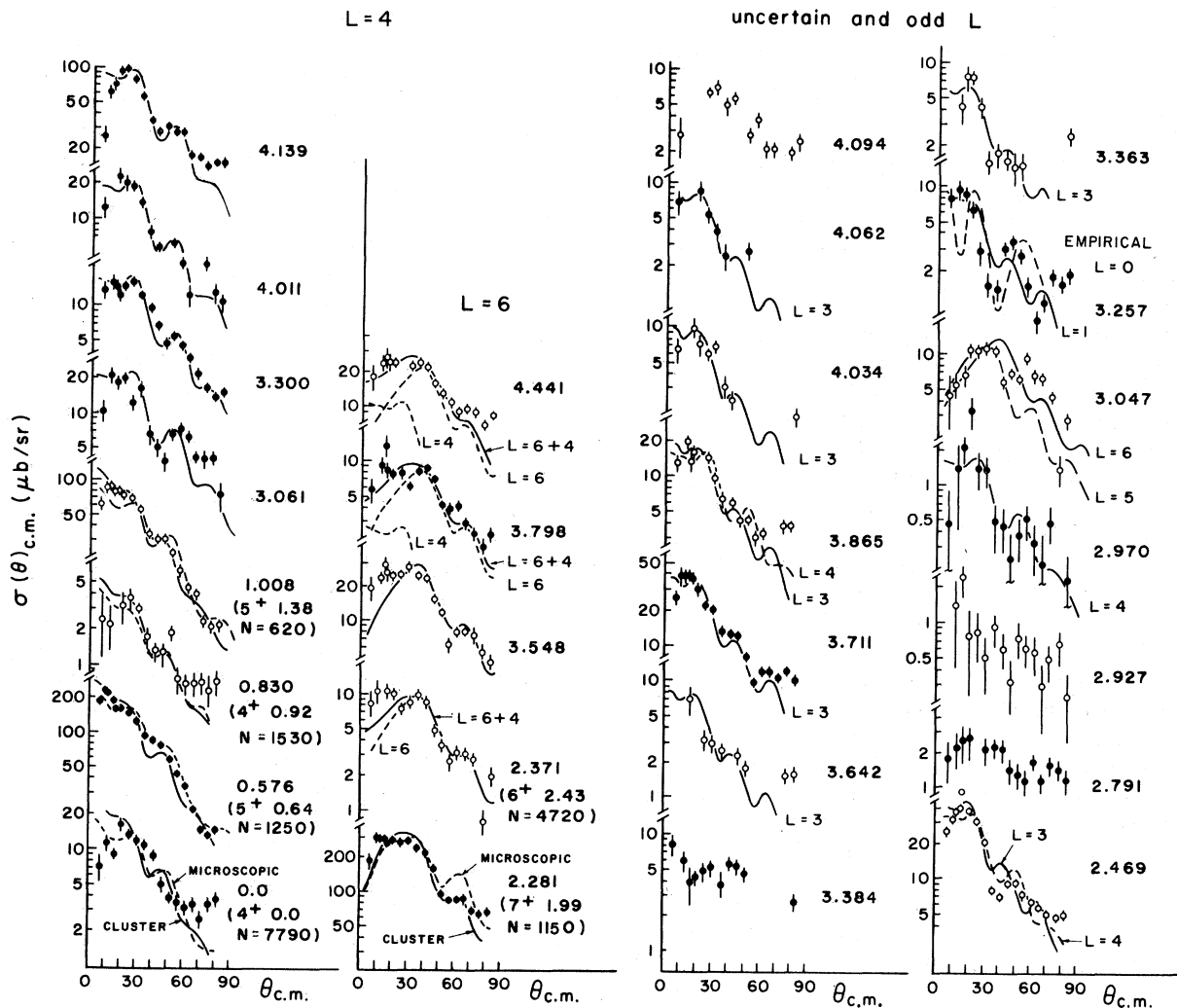


FIG. 5. Experimental  $(d, \alpha)$  cross sections and DWBA calculations for  $L=4$  and for uncertain and odd  $L$ . The absolute scale error is about 15%. Error bars shown represent statistical, monitoring, background, and multiplet separation errors added in quadratures. Those states with  $J^\pi$  given after the excitation energy are identified with McGrory's predicted levels. The predicted excitation energies and normalizations  $N(d, \alpha)$  are also given.

knowledge of the target thickness and is estimated at  $\pm 15\%$ .

Several puzzling variations appear in the experimental data. Angular distributions of identifiable  $L$  value undergo marked changes in shape from level to level necessitating extreme caution in spin assignments. For example, there appear to be two types of  $L=4$  angular distributions. The ground state is known to be  $4^+$  and must therefore be excited by pure  $L=4$ . The angular distribution to the 0.830-MeV state is similar to the ground state, and is fit somewhat better by the DWBA  $L=4$  curve than is the ground state. The 0.576-MeV level was excited with  $L=4$  in  $(\text{He}^3, p)^4$  and is believed to be  $5^+$  by identification with a predicted<sup>1-3</sup>  $5^+$  level in the vicinity. Its angular distribution in  $(d, \alpha)$  is almost identical to that of the 1.008-MeV level, but the angular distributions to these two states are quite different from those to the ground and 0.830-MeV states. If all are  $L=4$  it is possible that if the first pair had  $J^\pi=4^+$  and the second pair  $J^\pi=5^+$ , then an allowed  $L=6$  contribution could change the shape of the angular distribution, but neither known experimental nor DWBA  $L=6$  curves fall off as steeply as any of these do, and hence could not explain the differences seen. The variation does not seem to be a predictable configuration effect, since examination of theoretical transfer amplitudes reveals no obvious differences in the form factors for the two sets of states. There is the possibility that we are seeing a  $J$  dependence, for McGrory predicts  $4^+$  states at 0.0 and 0.92 MeV that can be identified with the first pair, and  $5^+$  states at 0.64 and 1.38 which can be identified with the second pair. An attempt was made to "mock up" a  $J$  dependence by varying the  $l \cdot s$  parameter  $\lambda$  for the single-particle wells in the form-factor calculation.  $\lambda$  was doubled from the usual value of 25 to a value of 50, and then was decreased to 0, but these changes only affected the magnitudes of the cross sections, without altering the angular distributions.

A similar effect is seen for  $L=2$  when comparing the 0.157- and 2.608-MeV angular distributions with those for 1.929, 2.059, and 2.221 MeV. The latter three show a well-defined second maximum at  $35^\circ$  as opposed to a mere shoulder on the first maximum for the first two. The DWBA calculations for  $L=2$  fit the 0.967- and 1.92-MeV levels, but show some disagreement with the other four, in particular with regard to the height of the second maximum and the behavior beyond  $60^\circ$  (compare for example the 1.929- and 2.059-MeV angular distributions). At higher excitations experimental angular distributions recognizable as  $L=2$  show "mere shoulder" or "well-defined second maximum" characteristics interchangeably. Hence an

energy dependence seems unlikely. DWBA calculations for individual configurations indicate that the presence of a strong  $f_{5/2}$  component in the form factor leads to angular distributions with a shoulder high up on the first maximum, but they do not explain the differences at higher angles seen in the experimental data. A configuration dependence is possible, but not enough  $2^+$  and  $3^+$  states are known with certainty to draw conclusions with regard to a possible  $2^+-3^+$   $J$  dependence. Similar variations of single- and double-peaked  $L=2$  curves were seen in  $\text{Zn}^{68}(d, \alpha)^{49}$  and  $\text{Cr}^{52}(d, \alpha)^{43}$ . Structure effects not predicted by the shell-model calculations used, or two-step processes,<sup>48</sup> may play some role in these moderately collective target nuclei and cause some of these unexpected variations.

$L=0$ . Direct  $\text{Ni}^{58}(d, \alpha) L=0$  transitions necessarily lead to  $1^+$  states and are generally distinguished by very structured angular distributions with two or more well-defined, deep minima. A survey of the data shows seven or eight angular distributions (see Fig. 4) which fit this description. Seven transitions have nearly identical shapes with minima near  $10^\circ$  and  $40^\circ$ , and one of these leads to a known  $1^+$  level at 1.718 MeV. Microscopic DWBA calculations predict shapes very close to those observed, but with the location of minima  $10-15^\circ$  out of phase. This phase error is reduced to less than  $5^\circ$  if cluster form factors are used. (Compare fits to the 1.718 level in Fig. 4.) Given the small cross sections and large momentum mismatch for  $L_{d,\alpha}=0$  and a strong sensitivity to details of the  $L=0$  form factor, we put more emphasis on experimental systematics than detailed DWBA fits in assigning  $L=0$  transfers. Five of the more strongly excited levels are assigned  $J^\pi=1^+$ . For two other levels we merely suggest ( $1^+$ ) because of the very small transfer cross section. The only other strongly structured angular distribution, that of the 3.257-MeV level, is unique. It is totally out of phase with all empirical and calculated  $L=0$  curves and does not agree with other DWBA curves either.

The observation of five to seven  $J^\pi=1^+$  levels below 3.5 MeV is very significant from the spectroscopic point of view. Vervier (who describes  $\text{Co}^{56}$  as a simple one-particle-one-hole nucleus) predicts only *one* such state, at 3.15 MeV, whereas the lowest  $1^+$  state lies at 1.718 MeV. McGrory, with his enlarged model space, predicts the lowest four  $1^+$  states with qualitatively correct strength and energies.

Calculations by Goode and Zamick<sup>5</sup> for  $1^+$  states of  $\text{Co}^{56}$  which also included two-particle-two-hole configurations yielded *eight*  $1^+$  levels below 3.8 MeV. That  $(d, \alpha)$  sees nearly this number in this

region suggests sizable two-hole-four-particle components in Ni<sup>58</sup>. It is surprising that the higher 1<sup>+</sup> states are no weaker than the low-lying ones (compare Table I). This indicates that there is enough configuration mixing in Co<sup>56</sup> to wipe out any distinction between states whose antecedents are  $\pi f_{7/2}^8$  and  $\pi f_{7/2}^6$  components of the Ni<sup>58</sup> ground-state wave function, since the latter are expected to be weaker (and lead to higher-lying Co<sup>56</sup> states) than the former.

Some variations in angular-distribution shape among the seven 1<sup>+</sup> transitions can be seen. All of them show a strong maximum at 25°, but a few almost lack the next one at 55°. Some of the variations in shape for a given  $L$  are probably due to errors in analyzing close-lying peaks, although the estimated error for this process is shown. For large variations from the norm or for well-separated peaks, the differences in shape are considered significant.

$L=2$ . We identify seventeen  $L=2$  angular distributions. Two of them populate known 2<sup>+</sup> and 3<sup>+</sup> levels, and are typical of two groups of  $L=2$  distributions which have a surprisingly disparate shape beyond the first maximum at 15°. Some data follow the DWBA curves exactly, but others have a second maximum which is shifted by ~10° towards smaller angles. Eight  $L=2$  transitions lead to states below 3 MeV, about the number predicted by McGrory for this region, but the one-particle-one-hole space of Vernier fails completely for excitations above 1.2 MeV. Even if a few of our suggested  $L=2$  assignments should turn out to be incorrect, the number of  $L=2$  transitions of reasonable strength ( $8 \mu\text{b/sr} \leq \sigma_{\text{max}} \leq 32 \mu\text{b/sr}$  with the exception of three states of  $\sigma_{\text{max}} \geq 80 \mu\text{b/sr}$ ) is so large as to require  $\pi f_{7/2}$  hole components in Ni<sup>58</sup> for their explanation.

$L=4$ . Eight angular distributions have been assigned  $L=4$ . At higher excitations two more states appear to be either  $L=3$  or 4. The ground state and 0.830-MeV  $L=4$  transitions are fitted relatively poorly. Although the 0.830-MeV transition is weak and could have sizable contributions from nondirect processes, the same cannot be said of the ground state, whose angular distribution is similar.

$L=6$ . Five fairly certain  $L=6$  angular distributions are seen. Their shapes agree well with each other and with the DWBA curve except below 20°. This agreement is especially satisfying in view of previous difficulties<sup>20,43</sup> with  $L=6$  in  $(d, \alpha)$ . The dominant  $L=6$  transition is expected to lead to the  $(\pi f_{7/2}, \nu f_{7/2})^{-1}_{7+}$  state. Its relative strength and energy compare well with McGrory's calculation. Any  $J^\pi = 6^+$  state would be weakened by the forbiddenness of  $(f_{7/2})^2$  pickup.

Fits to the 2.371-, 3.548-, 3.798-, and 4.441-MeV transitions would be improved by  $L=4$  admixtures as indicated in the curves for the latter two. However, the  $L=6$  curve for the 7<sup>+</sup> state (where there can be no  $L=4$  admixture) has a similar small angle deficiency, and the improved fit with addition of  $L=4$  does not necessarily indicate 5<sup>+</sup> assignments for these levels.

*Odd and uncertain L.* There are a number of transitions for which  $L$  identifications are very uncertain. Included among them are those angular distributions that resemble DWBA calculations for odd- $L$  values. In view of the difficulties with DWBA predictions for known even- $L$  transfers, odd- $L$  assignments are to be viewed as tentative suggestions.  $(d, \alpha)$  selection rules for a 0<sup>+</sup> target dictate that odd- $L$  values will excite negative-parity states. By far the strongest negative-parity states expected in this experiment are those formed by  $f_{7/2}-d_{3/2}$  pickup, with  $5^- \leq J^\pi \leq 2^-$  and  $5 \leq L \leq 1$ . We see seven possible  $L=3$  levels at excitations of 2.469 MeV and above.

#### IV. DISCUSSION OF INDIVIDUAL LEVELS

##### A. General Considerations

In this section Co<sup>56</sup> levels are considered individually, and experimental data of the present and previous experiments are correlated and compared with theoretical treatments when these are available. Spin and parity assignments, or sometimes limits, and our conclusions about spectroscopic and configurational details are also presented. We will repeatedly refer to and compare our results with several spectroscopically interesting experiments that have increased our understanding of Co<sup>56</sup>. Among these are studies of Wells, Blatt, and Meyerhof,<sup>6</sup> Jenkins and Meyerhof,<sup>7</sup> Ohnuma, Hashimoto, and Tomita,<sup>8</sup> and Piluso, Wells, and McDaniels,<sup>9</sup> who used a variety of  $\gamma$  spectroscopic techniques [prompt- and delayed-coincidence spectra, angular correlations, conversion electron spectra, Ge(Li) spectra] to arrive at unique conclusions about  $J^\pi$  of four of the five levels that are populated in Ni<sup>56</sup>  $\beta^+$  decay. These experimenters tried to fit Co<sup>56</sup> into the one-particle-one-hole pattern, and Wells<sup>1</sup> and Ohnuma, Hashimoto, and Tomita<sup>8</sup> deduced the necessity for some configuration mixing, but all were seriously hampered in their analyses by the incorrect assignments of 1<sup>-</sup>, 2<sup>±</sup> for the 1.450-MeV level. Among our precursors in  $(d, \alpha)$  investigations are Bjerregard *et al.*<sup>12</sup> and Belote, Dorenbusch, and Rappaport<sup>10</sup> who at 4 and 7 MeV, respectively, observed a total of 38 Co<sup>56</sup> levels. Hjorth<sup>13</sup> did  $(d, \alpha)$  spectroscopy of Co<sup>56</sup> at 15 MeV and suggested  $L$  values for 15 levels. Laget and Gastebois<sup>4</sup> investigated

$(d, \alpha)$  at 12 MeV. The extensive 18-MeV ( $\text{He}^3, p$ ) study by the same authors led to  $L$  suggestions for 16 levels.

The ( $\text{He}^3, p$ ) level strengths of Laget and Gastebois, or our higher-resolution spectra when necessary, will be used below for comparison with present  $(d, \alpha)$  spectra, ( $\text{He}^3, t$ ) spectra of Roos and Goodman,<sup>14</sup> and  $(p, \text{He}^3)$  spectra of Bruge *et al.*<sup>15</sup> Qualitatively, comparison of  $\text{Ni}^{58}(d, \alpha)$ ,  $\text{Fe}^{54}(\text{He}^3, p)$ , and  $\text{Fe}^{56}(\text{He}^3, t)$  spectra leading to  $\text{Co}^{56}$  should give useful information on configuration mixing in this nucleus. For example, the strongest states in the ( $\text{He}^3, t$ ) spectrum should be largely  $(\pi f_{7/2}^{-1}, \nu f_{7/2}^{-1}, p_{3/2}^2)$  and  $(\pi f_{7/2}^{-2}, p_{3/2}, \nu p_{3/2})$  if the common assumption is made that that reaction goes primarily by charge exchange. Furthermore these states usually should be weak in ( $\text{He}^3, p$ ), as for the  $\text{Fe}^{54}$  ground state the  $f_{7/2}$  neutron shell is filled. The ( $\text{He}^3, p$ ) reaction, however, will populate states of the  $(\pi f_{7/2}^{-1}, \nu p_{3/2})$ ,  $(\pi f_{7/2}^{-1}, \nu f_{5/2})$ , and  $(\pi f_{7/2}^{-1}, \nu p_{1/2})$  configurations more strongly than ( $\text{He}^3, t$ ), and both of these reactions will excite  $\pi f_{7/2}^{-2}$  configurations more strongly than  $(d, \alpha)$ . Many levels are seen strongly in two or all three of these spectra, indicating appreciable configuration mixing. Particular examples will be discussed below.

Theoretical studies of  $\text{Co}^{56}$  have been made by Vervier<sup>2</sup> and McGrory,<sup>3</sup> and it will be illuminating to compare our final conclusions with their predictions. A level-by-level comparison will be made with McGrory's predicted  $(d, \alpha)$  transition amplitudes for about 15 states in those cases where matching of predicted and actual levels is possible. Where the identifications are straightforward, angular distribution strengths were calculated with McGrory's suggested transfer amplitudes for each contributing configuration. Confidence in matching the lowest levels is high, but at higher excitations the correspondence of predicted and observed states is more uncertain. Predicted strengths were calculated using a normalization of  $N(d, \alpha) = 900$  for the output of the code DWUCK.

When  $L$  is known,  $(d, \alpha)$  selection rules for  $0^+$  targets limit  $J$  to  $J = L, L \pm 1$ , although for states in this experiment where two  $L$  values are allowed the relevant  $LS$ - $JJ$  transformation coefficients and experience indicate that the lower  $L$  always predominates. Hence we will consider  $J = L, L + 1$  as more likely spins, while not ruling out  $J = L - 1$  entirely. A good indication of whether spins of low-lying levels are even or odd can sometimes be obtained from the ratio of  $\text{Ni}^{58}(d, \alpha)\text{Co}^{56}$  to  $\text{Ni}^{58}(p, \text{He}^3)\text{Co}^{56}$  cross sections, since under the direct reaction assumption  $(p, \text{He}^3)$  leading to even  $J^+$  states is allowed to pick up a singlet deuteron whereas  $(d, \alpha)$  is not, and  $(p, \text{He}^3)$  leading to even  $J^+$  states is also allowed to pick up a  $p$ - $n$  pair in the  $(l_j)^2$

configuration, which  $(d, \alpha)$  cannot do either. Thus  $0^+$  states are not excited in this  $(d, \alpha)$  experiment, while they are easily populated in  $(p, \text{He}^3)$  or  $(\text{He}^3, p)$  transfers. The absence of  $0^+$  states in  $(d, \alpha)$  spectra (compare the 1.450-MeV excitation in Figs. 1 and 2) is a necessary condition for use of direct- $(d, \alpha)$ -transfer selection rules.

The transition from a  $0^+$  target to  $J_{\text{odd}}^+$  and  $J_{\text{even}}^-$  states requires triplet deuteron transfer in  $(p, \text{He}^3)$  and  $(d, \alpha)$ . Hence there will be a constant strength ratio for these states in the two reactions except for slowly varying functions of  $L$ ,  $Q$ , and bombarding energy  $E$ . On the other hand, excitation of  $J_{\text{even}}^+$  and  $J_{\text{odd}}^-$  states (other than  $0^+$ ) will proceed by triplet plus singlet transfer for  $(p, \text{He}^3)$ , while  $(d, \alpha)$  remains restricted to triplet transfer. Since triplet and singlet strengths add incoherently (in the absence of an  $l \cdot s$  interaction), the ratio  $\sigma(d, \alpha)/\sigma(p, \text{He}^3)$  for these states ought to be noticeably smaller than its value for  $J_{\text{odd}}^+$  and  $J_{\text{even}}^-$  states. If a  $J_{\text{even}}^+$  state has an almost pure  $(l_j)^2$  configuration,  $\sigma(d, \alpha)/\sigma(p, \text{He}^3)$  will be very small. If it has nearly equal amounts of  $(j)_{\text{even}}^2$  and  $(j_1 j_2)_{\text{even}}$  components, singlet-transfer amplitudes may add constructively, in which case this ratio will still be small; or destructively, in which case this ratio will approach that for  $J_{\text{odd}}^+$  and  $J_{\text{even}}^-$ .

Therefore, if a relative  $(d, \alpha)$  cross section is very much smaller than the corresponding  $(p, \text{He}^3)$

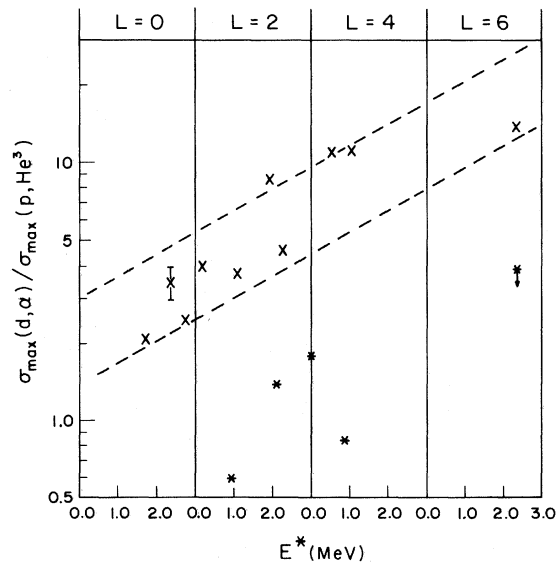


FIG. 6. Maximum  $(d, \alpha)$  cross section divided by maximum  $(p, \text{He}^3)$  cross section (Ref. 17) for those levels from Table I where  $L$  determination was possible. Previously known  $J^\pi$  values are included.  $\times$  indicates odd  $J$  as most likely,  $*$  indicates even  $J$ . The arrow pointing up (down) indicates that the ratio shown is the minimum (maximum) possible, insofar as can be judged from the  $(p, \text{He}^3)$  spectrum.



cross section, the final state must have  $J=\text{even}$ , usually with  $(l_j)^2$  as a dominant configuration [or be of different isospin, in which case the  $(d, \alpha)$  cross section should go to zero]. This rule allows some definite  $J=L$  assignments for states where  $L(p, \text{He}^3)$  and the related cross sections are reliably known. If the observed cross-section ratio for a level is relatively small, the level is most likely  $J=\text{even}=L$ , but if the ratio is "normal" no definite conclusions may be drawn, as it may be either  $J_{\text{odd}}^+$  or  $J_{\text{even}}^+$  with small singlet transfer strength.

For the data at hand there is a definite grouping of  $(d, \alpha)/(p, \text{He}^3)$  ratios (see Fig. 6). All ratios for known  $J_{\text{odd}}^+$  states (plotted vs  $L$  and  $Q$ ) lie in the narrow band indicated by the dashed lines, and all known  $J_{\text{even}}^+$  states lie lower by factors of 2 or more, in agreement with expectations. Hence for unknown levels for which the appropriate information is available, the low ratios indicate  $J_{\text{even}}^+$  and usually an  $(l_j)^2$  configuration. For the normal ratios we can deduce that the states are either  $J_{\text{odd}}^+$  or at least have no dominant  $(l_j)^2_{J_{\text{even}}^+}$  component.

#### B. Individual Levels

1. *Ground state,  $E_x=0.0$ ,  $J^\pi=4^+$ .* All experimental evidence is consistent with the original  $J^\pi=4^+$  assignment based on  $\beta$ - $\gamma$  decay<sup>6</sup> and hyperfine structure in paramagnetic resonance.<sup>47</sup> Elementary shell-model considerations suggest  $(\pi f_{7/2}^{-1}, \nu p_{3/2})$  as the dominant configuration. The calculations of McGrory predict a  $4^+$  ground state and suggest that in  $(d, \alpha)$   $(f_{7/2}, p_{3/2})$  is in fact the strongest configuration transferred, but this is the result of the forbiddenness of  $[j^2]_{J_{\text{even}}}$  transfer. Although in  $(d, \alpha)$  the observed strength of this level is weak, it is still roughly eight times more strongly excited than predicted. The predicted weakness is due to cancellation of the  $(f_{7/2}, p_{3/2})$  and  $(f_{7/2}, p_{1/2})$  transfer amplitudes. Two things suggest that the ground state has a large  $(\pi f_{7/2}^{-1}, \nu f_{7/2}^{-1})$  component: (1) It is most strongly excited, relative to nearby levels, in  $\text{Fe}^{56}(\text{He}^3, t)$ ; and (2) it is of even spin and has a small  $\sigma(d, \alpha)/\sigma(p, \text{He}^3)$  ratio (Fig. 6).

2.  *$E_x=0.157$  MeV,  $3^+$ .* The 0.157-MeV level of  $\text{Co}^{56}$  is appreciably populated in all transfer reactions studied. Its angular distribution was identified as  $L=2$  in  $(d, \alpha)$ ,  $(\text{He}^3, p)$ , and  $(p, \text{He}^3)$ , permitting a  $2^+$ ,  $3^+$ , or  $(1^+)$  spin. This state has a normal  $\sigma(d, \alpha)/\sigma(p, \text{He}^3)$  ratio which is consistent with  $J=\text{odd}$ , and the  $3^+$  assignment of previous  $\gamma$ -ray work.<sup>6-9</sup> McGrory's wave functions predict a strong  $L=2$  transition (with an almost negligible admixture of  $L=4$ ) to a  $3^+$  level at 0.23-MeV excitation, and its predicted strength about equals

the observed strength of this level. Shell-model calculations give  $(f_{7/2}, p_{3/2})$  as the strongest configuration transferred. The importance of this configuration in the ground and 0.157-MeV states has also been deduced from  $\gamma$  transition characteristics.<sup>1</sup>

3.  *$E_x=0.576$  MeV ( $5^+$ ).* This level is one of the strongest seen in  $(d, \alpha)$  and  $(p, \text{He}^3)$ , but is only weakly excited in  $(\text{He}^3, p)$  and  $(\text{He}^3, t)$ . The  $10^\circ$  peak in the  $(d, \alpha)$  angular distribution had previously been taken as evidence for some  $L=2$  admixture,<sup>48</sup> but the good  $L=4$  fit obtained with the new well-matching calculations invalidates the earlier argument. The 0.576-MeV level is excited with a normal  $\sigma(d, \alpha)/\sigma(p, \text{He}^3)$  ratio, consistent with  $J=\text{odd}$ .  $L=4$  angular distributions are seen for this state in  $(\text{He}^3, p)$  and  $(p, \text{He}^3)$ . The 15-MeV  $(d, \alpha)$  data<sup>13</sup> were also assigned  $L=4$ . These  $L$  assignments support  $4^+$  or  $5^+$ , but are not inconsistent with  $3^+$ . Early  $5^+$  assignments for this state were primarily based on theoretical predictions of a  $5^+$  state in this vicinity. McGrory, too, predicts a  $5^+$  level of about the observed  $L=4$  strength at 0.64 MeV. On the basis of this good spectroscopic agreement we also suggest  $5^+$ .

4.  *$E_x=0.830$  MeV ( $4^+$ ).* This state is seen weakly in  $(d, \alpha)$ ,  $(p, \text{He}^3)$ , and  $(\text{He}^3, t)$  and very weakly in  $(\text{He}^3, p)$ . The  $(d, \alpha)$  angular distribution is well fitted by an  $L=4$  curve of about the strength predicted by McGrory for a  $4^+$  level near 0.92 MeV. This is the first good  $L=4$  fit for this level in any transfer experiment. The  $\sigma(d, \alpha)/\sigma(p, \text{He}^3)$  ratio is very low, indicating  $J=\text{even}$ , and we suggest that this level has  $J^\pi=4^+$ . McGrory's calculations predict that the largest component of the  $(d, \alpha)$  transfer amplitude is  $(f_{7/2}, f_{5/2})$ , but it is largely canceled by the  $(f_{7/2}, p_{1/2})$  term.

5.  *$E_x=0.967$  MeV,  $2^+$ .* This state is moderately excited in all four reactions. It is poorly resolved from the 1.008-MeV state in  $(p, \text{He}^3)$ , but its angular distribution was recognized as primarily  $L=2$ . Our DWBA cluster  $L=2$  fit is not good, although the microscopic fit is somewhat better. This state is much stronger in  $(p, \text{He}^3)$  than  $(d, \alpha)$  and so our assignment would be  $J=\text{even}$ , i.e.,  $2^+$ . It also participates in the  $\gamma$  cascade from  $\text{Ni}^{56} \beta^+$  decay, and through  $\gamma$  spectroscopy has been assigned to be a  $2^+$  state of primarily the same configuration as the ground state. McGrory predicts a  $2^+$  state, excited primarily by transfer of an  $(f_{7/2}, p_{3/2})$  pair, at 0.99 MeV, and presumably this is that state. Its experimental strength is about half that predicted. We feel that the suggested  $3^+$  assignment in Ref. 17 is not tenable.

6.  *$E_x=1.008$  MeV ( $5^+$ ).* This level is excited weakly in  $(\text{He}^3, p)$ . In other particle-transfer studies of modest resolution it was lost in the tail

of the 0.967 level. However, it is excited strongly in  $(d, \alpha)$  with an  $L=4$  angular distribution very similar to the 0.576-MeV ( $5^+$ ) state. Its  $(d, \alpha)$  strength is consistent with  $J=\text{odd}$ , and is about that predicted for a  $5^+$  state at 1.38 MeV. Its  $(d, \alpha)$  strength comes, according to McGrory, from constructive interference of  $(f_{7/2}, p_{3/2})$ ,  $(f_{7/2}, f_{7/2})$ , and  $(f_{7/2}, f_{5/2})$  transfer amplitudes. One former tentative assignment<sup>1</sup> for this state was  $3^+$  based on the prediction of such a level near this energy.<sup>2</sup> A claim<sup>17</sup> that an  $L=2$  angular distribution is seen in  $(p, \text{He}^3)$  must be questioned, because this state is not well resolved from the 0.967-MeV ( $L=2+4$ ) transition in that (45-keV resolution) experiment. Hjorth<sup>13</sup> earlier proposed  $5^+$  for this state after classifying as  $L=4$  the combined  $(d, \alpha)$  angular distributions of this and the 0.967-MeV level. Our suggested assignment also is ( $5^+$ ).

7.  $E_x = 1.112 \text{ MeV}$  ( $3^+$ ). This state is excited very weakly in  $(\text{He}^3, t)$ , weakly in  $(\text{He}^3, p)$  and  $(p, \text{He}^3)$ , and moderately in  $(d, \alpha)$ . The  $\sigma(d, \alpha)/\sigma(p, \text{He}^3)$  ratio agrees with  $J=\text{odd}$ . Although the DWBA  $L=2$  curve (dotted line) does not reproduce this angular distribution well, the fit of the empirical  $L=2+4$  curve derived from nearby states is evidence for  $J=3$ .  $\sigma(d, \alpha)$  is also very close to that predicted for a  $3^+$  level at 1.16 MeV. If this state were  $2^+$  its apparent nonparticipation in the  $\beta$ - $\gamma$  cascade would be difficult to explain. Previous  $J^\pi$  suggestions for this state have been  $3^+$ , based on  $L=2$  in  $(d, \alpha)$ ,<sup>13</sup> and  $4^+$ ,<sup>1,2,17</sup> based on shell-model calculations. McGrory predicts a  $3^+$  state at 1.16 MeV to be excited with almost pure  $L=2$ , predominantly by  $(f_{7/2}, f_{5/2})$  transfer. The apparent strong  $L=4$  admixture is unusual and unpredicted.

8.  $E_x = 1.450 \text{ MeV}$ ,  $0^+$ . This state, the antianalog to the  $\text{Fe}^{56}$  ground state, is forbidden in  $(d, \alpha)$  and in fact is indistinguishable from the background in all of our  $(d, \alpha)$  spectra. It is appreciably excited, however, in  $(\text{He}^3, p)$ ,  $(p, \text{He}^3)$  (both with  $L=0$ ), and  $(\text{He}^3, t)$ . Recent experiments,<sup>4,10</sup> including the present one, appear to have successfully refuted earlier suggestions of  $(1^-, 2^+)$  based primarily on  $\gamma$ - $\gamma$  coincidences that did not quite look isotropic. Roos and Goodman<sup>14</sup> have suggested that there may be a  $1^-$  state within a few keV of this one, since its  $(\text{He}^3, t)$  angular distribution agrees with known  $l=1$  shapes. However, several other  $(\text{He}^3, t)$  transitions to  $0^+$  antianalog states have given  $l=1$  shapes,<sup>49</sup> and no evidence for a  $1^-$  state in this vicinity is seen in this experiment. The antianalog state is predicted by McGrory to lie at about 2 MeV, which is a larger deviation from its actual location than for most other predicted levels that could be matched with observed

ones.

9.  $E_x = 1.718 \text{ MeV}$ ,  $1^+$ . This level is seen rather strongly in  $(\text{He}^3, t)$  and  $(\text{He}^3, p)$  and is somewhat weaker in  $(d, \alpha)$  and  $(p, \text{He}^3)$ . The  $L=0$  angular distribution in  $(d, \alpha)$  and the  $L=0+2$  in  $(\text{He}^3, p)$  and  $(p, \text{He}^3)$  confirm the assignment  $1^+$  originally made by analysis of  $\text{Ni}^{56}$  electron capture leading to this state. It has previously been recognized<sup>2,5,10</sup> that this level has a large two-particle-two-hole component which cannot be excited in the  $\beta^+$  decay of the doubly closed  $f_{7/2}$  shell component of the  $\text{Ni}^{56}$  ground state. It is seen in  $(d, \alpha)$  with approximately the strength predicted for a  $1^+$  state at 1.68 MeV.

10.  $E_x = 1.929 \text{ MeV}$ ,  $3^+$  ( $2^+$ ). This level is seen strongly in all reactions except  $(\text{He}^3, t)$ . The  $(\text{He}^3, p)$  angular distribution has been identified as  $L=2$ . In  $(d, \alpha)$  this is the lowest (and strongest) of three consecutive  $L=2$  states. Its  $\sigma(d, \alpha)$  to  $\sigma(p, \text{He}^3)$  ratio is normal; hence a  $3^+$  assignment is allowed. Previous experimenters<sup>4,13</sup> had been unable to decide between  $2^+$  and  $3^+$ . The state's relative weakness in  $(\text{He}^3, t)$  suggests dominant  $(\pi f_{7/2}^{-1}, \nu p_{3/2}, f_{5/2}, \text{ or } p_{1/2})$  structure. McGrory predicts an  $L=2$  transition with  $\frac{2}{3}$  the observed strength of this state to a  $3^+$  level at 2.08 MeV. The considerable  $(d, \alpha)$   $L=2$  strength is explained as constructive interference of  $(f, f)$ ,  $(f, p)$ , and  $(p, p)$  pickup from  $\text{Ni}^{56}$  in almost equal amounts.

Angular distributions to levels above 2 MeV in excitation have been fit with calculations assuming  $E_x = 3 \text{ MeV}$ . The difference between the 1- and 3-MeV calculations is small, but not insignificant, as exemplified by the difference between the 1.929- and 2.059-MeV level fits.

11.  $E_x = 2.059 \text{ MeV}$ ,  $2^+$  ( $3^+$ ). The 2.059-MeV level is excited moderately in all reactions, but with a very small  $\sigma(d, \alpha)/\sigma(p, \text{He}^3)$  ratio, which suggests  $J=\text{even}$ .  $(p, \text{He}^3)$  and  $(\text{He}^3, p)$  have been fitted by  $L=2$ . Our DWBA  $L=2$  curve gives a good fit to the data, and so our preferred assignment is  $2^+$ . McGrory predicts a  $2^+$  state at 2.09 MeV with a strength of about twice that observed for this state.

12.  $E_x = 2.221 \text{ MeV}$ ,  $3^+$  ( $2^+$ ). Excited very weakly in  $(\text{He}^3, p)$ , weakly in  $(p, \text{He}^3)$ , and moderately in  $(d, \alpha)$  and  $(\text{He}^3, t)$ , this level is also easily recognized as  $L=2$ . The  $\sigma(d, \alpha)/\sigma(p, \text{He}^3)$  ratio is normal and so  $3^+$  is a slightly preferred assignment. The next  $3^+$  level of McGrory is at 2.44 MeV, and we suggest a correspondence to that state, although it is only  $\frac{1}{3}$  as strong as predicted.

13.  $E_x = 2.281 \text{ MeV}$ ,  $7^+$ . This is the strongest low-lying state in  $(d, \alpha)$  and  $(\text{He}^3, t)$ . It is very weak in  $(\text{He}^3, p)$ . Its strong  $(p, \text{He}^3)$  angular distribution was identified as  $L=6$ , and its  $(d, \alpha)$  angular distribution, too, is unquestionably  $L=6$  al-

though there are minor disagreements with the DWBA curve. The  $(d, \alpha)$  to  $(p, \text{He}^3)$  ratio indicates  $J = \text{odd}$ . Its great strength immediately suggests a  $(\pi f_{7/2}, \nu f_{7/2})_{7^+}$  transfer: (1) On statistical grounds all odd- $J$  states of this configuration should be strong, and  $7^+$  should be the strongest of these; (2) the strength of the angular momentum vectors adding to  $J = 7$  is not fractionated among other states; (3) the weakness in  $(\text{He}^3, p)$  supports assignment of a predominant  $(f_{7/2})^{-2}$  configuration; and (4) comparison of this state's location in Co<sup>56</sup> and Co<sup>58</sup> suggests  $7^+$  also, as has been pointed out by Hjorth.<sup>13</sup> McGrory's strong  $7^+$  state is predicted for 1.99 MeV, and as the strongest  $(d, \alpha)$  transition, as observed.

14.  $E_x = 2.301 \text{ MeV } (2^+, 3^+)$ . In  $(\text{He}^3, p)$  a level at  $\sim 2.296$  MeV is excited with  $L = 2$ . Reconciliation of this  $L$  with the  $7^+$  assignment for the previous state would be difficult. Several experimenters have suggested a close-lying doublet in this vicinity, and our  $(\text{He}^3, p)$  data (see Fig. 2) resolve the doublet. In  $(d, \alpha)$  we see a low-energy tail on the 2.281 peak slightly broader than the characteristic low-energy tail of other very tall peaks seen in the spectrograph data. We could not, of course, extract a  $(d, \alpha)$  angular distribution for this state, and so we rely upon the observed  $L = 2$  transition for  $(\text{He}^3, p)$  for a suggested  $2^+$  or  $3^+$  assignment. This state is not resolved from the 2.281-MeV level in  $(p, \text{He}^3)$  or  $(\text{He}^3, t)$ .

Above this energy the level density increases and matching of states in four different reaction spectra, each with slightly different energy scale, becomes difficult. Therefore we must rely less on this method of spectroscopy and make more tentative assignments.

15.  $E_x = 2.357 \text{ MeV } (1^+)$ . One or both members of the 2.357-2.371 doublet is excited moderately to weakly in  $(\text{He}^3, p)$ ,  $(\text{He}^3, t)$ , and  $(p, \text{He}^3)$ , but it is difficult to tell which. The 2.357-MeV member is weak in  $(d, \alpha)$ . Its angular distribution is apparently  $L = 0$ , leading to a  $(1^+)$  assignment. Some of the disagreement between data and DWBA curve might have arisen from imperfect separation of the doublet in our analysis, but the  $L = 0$  pattern is clear. McGrory predicts a  $1^+$  level at 2.45 MeV with somewhat more than half the strength of this level.

16.  $E_x = 2.371 \text{ MeV } (6^+, 5^+, 7^+)$ . This level is the first of several which are fitted reasonably well by  $L = 6$  but are fitted somewhat better by  $L = 6 + (4)$ . As discussed earlier, the apparent need for some  $L = 4$  admixture seems to be a shortcoming of our DWBA calculations; hence a  $5^+$  assignment is not called for. The  $(d, \alpha)$  to  $(p, \text{He}^3)$  ratio points to an even- $J$  assignment, but the lowest  $6^+$  level of McGrory (at 2.43 MeV) is predicted to be somewhat weaker than this state ( $\sigma_{\text{max}} \sim 2 \mu\text{b/sr}$ ). The sec-

ond  $7^+$  state of McGrory is predicted at 3.5 MeV, making that assignment unlikely.

17.  $E_x = 2.469 \text{ MeV}$ . The situation with respect to this state is also unclear. In  $(\text{He}^3, p)$  a state is seen in this region with  $L = 4$ , and our high-resolution  $(\text{He}^3, p)$  spectra show an isolated state here with a  $15\text{--}30^\circ$  cross-section ratio favoring  $L = 4$ . In  $(p, \text{He}^3)$ , however, a state here was classified as  $L = 0$ . A strong angular distribution closely resembling  $L = 3$ , but conceivably  $L = 4$ , is seen in the present  $(d, \alpha)$  work. No final conclusions can be drawn.

18.  $E_x = 2.608 \text{ MeV } (2^+, 3^+)$ . This level is the first of what we believe to be a quadruplet of states. Separation of peaks for cross-section determination, particularly for the central doublet, is less reliable here than elsewhere. Nevertheless we believe that  $L$  values are correct. This state is seen with a clear  $L = 2$  angular distribution in  $(d, \alpha)$ . In  $(p, \text{He}^3)$  a state at 2.626 MeV is seen with  $L = 2$ .

19.  $E_x = 2.634 \text{ MeV } (1^+)$ . A moderately well fitted  $L = 0$  angular distribution of intermediate strength is seen in  $(d, \alpha)$  for this level, leading to  $J^\pi = 1^+$ . This state appears to be appreciably excited in  $(\text{He}^3, t)$  also, suggesting  $(\pi f_{7/2}^{-1}, \nu f_{7/2}^{-1})$  as a significant configuration. It has not been resolved in the  $(\text{He}^3, p)$  or  $(p, \text{He}^3)$  spectra. McGrory predicts a  $1^+$  level at 2.72 MeV, but it could well be one of the higher  $L = 0$  transitions we see, several of which are excited with comparable strength.

20.  $E_x = 2.647 \text{ MeV } (1^+)$ . This level also appears to have  $L = 0$  judging from our DWBA fit. Although the familiar rise at  $\theta = 0^\circ$  is absent, the resemblance to other  $L = 0$  angular distributions is fair to good. The 2.634-2.647-MeV doublet has not been identified as such before. The combined angular distribution of the two states (not shown) also looks like  $L = 0$ , suggesting that there is little or no  $L \neq 0$  "impurity," but in view of the deficiencies of the fits our  $1^+$  suggestions are only tentative.

21.  $E_x = 2.666 \text{ MeV } (2^+, 3^+)$ . A good  $L = 2$  angular distribution is seen for this rather weak state. Identification with corresponding peaks in other reactions is difficult.

22.  $E_x = 2.728 \text{ MeV } (1^+)$ . This level is seen very strongly in  $(\text{He}^3, t)$  and moderately in both deuteron pickup reactions.  $L = 0 + 2$  has been recognized in  $(p, \text{He}^3)$ , and our  $(d, \alpha)$  angular distribution is dominated by  $L = 0$ , giving  $J^\pi = 1^+$ . The  $(\text{He}^3, t)$  strength suggests  $(\pi f_{7/2}^{-1}, \nu f_{7/2}^{-1})$  as an important configuration. McGrory's transfer amplitudes for a  $1^+$  state at 2.72 with half the strength of the 2.728 show  $(\pi f_{7/2}, \nu f_{7/2})$  transfer 85 times stronger than any other contributing configuration, and hence experimental and theoretical determina-

tions of the structure of the 2.728-MeV state support each other.

23-25.  $E_x = 2.791, 2.927, 2.970$  MeV. Quite weak, and structureless angular distributions are seen for these levels. Hence no assignments are possible.

26.  $E_x = 3.061$  MeV,  $4^+ (5^+)$ . This angular distribution is nicely fitted by the  $L=4$  curve, and this state may correspond to a  $(p, \text{He}^3)$  transition of  $L=4$  seen at 3.048 MeV.

27.  $E_x = 3.075$  MeV,  $2^+, 3^+$ . Seen in  $(d, \alpha)$  and  $(\text{He}^3, p)$  with well-identified  $L=2$  angular distributions, this level gets a  $2^+$  or  $3^+$  assignment.

### C. Higher States

Table I summarizes suggested or tentative  $L$  assignments for a large number of states above 3 MeV. However, uncertainties in experimental energy scales and the low resolution in most earlier work make comparison with other experiments futile. Similarly, McGrory's shell-model space obviously misses many states for  $E \geq 3$  MeV. Hence a detailed discussion of these states does not seem warranted at this time. There is also the increasingly larger probability of unresolved doublets in our data (see Fig. 1). There is good reason to believe that several states in this region have negative parity, and the distinction of  $L=3$  from  $L=4$  solely on the basis of DWBA curves is at best tentative.

However, one very strong state measured by us as  $E_x = 5.146$  MeV stands out and may merit special consideration. It was first seen by Hjorth<sup>13</sup> at 5.18 MeV and tentatively assigned  $L=4$ . For the present study it was too high in excitation for us to extract an angular distribution, and the data given by Bruge *et al.* give no clue as to the  $L$  value for a very strong level seen at 5.090 MeV. This state has also been seen by Sherr<sup>17</sup> at 5.116 MeV. Despite the difference in excitation-energy assignments of the three groups, this distinctive peak must belong to the same two-hole state. It is not among the strong peaks seen by Lu *et al.*<sup>50</sup> in  $\text{Fe}^{54}(\alpha, d)$ .

### V. GENERAL DISCUSSION AND SUMMARY

The simplest interpretation of low-lying  $\text{Co}^{56}$  levels is given by the one-particle-one-hole approach as used by Vervier, who computed locations for 12 expected states of this type. Vervier implicitly included some consequences of admixtures of configurations outside his simple  $(\pi f_{7/2}^{-1}, \nu p_{3/2}, f_{5/2}, p_{1/2})$  space by deducing effective matrix elements from actual level locations in  $\text{Co}^{56}$  and other nuclei. Although his wave functions were able to give a reasonable fit to the lowest  $\text{Co}^{56}$  lev-

els, they are seriously limited by neglect of two-particle-two-hole components. Since states known to be of this configuration (for example the  $0^+$ ,  $1^+$ , and  $7^+$  states at 1.450, 1.718, and 2.281 MeV, respectively) appear well below the highest levels predicted by Vervier, this configuration must admix appreciably with one-particle-one-hole states.

The calculations of McGrory go quite a bit fur-

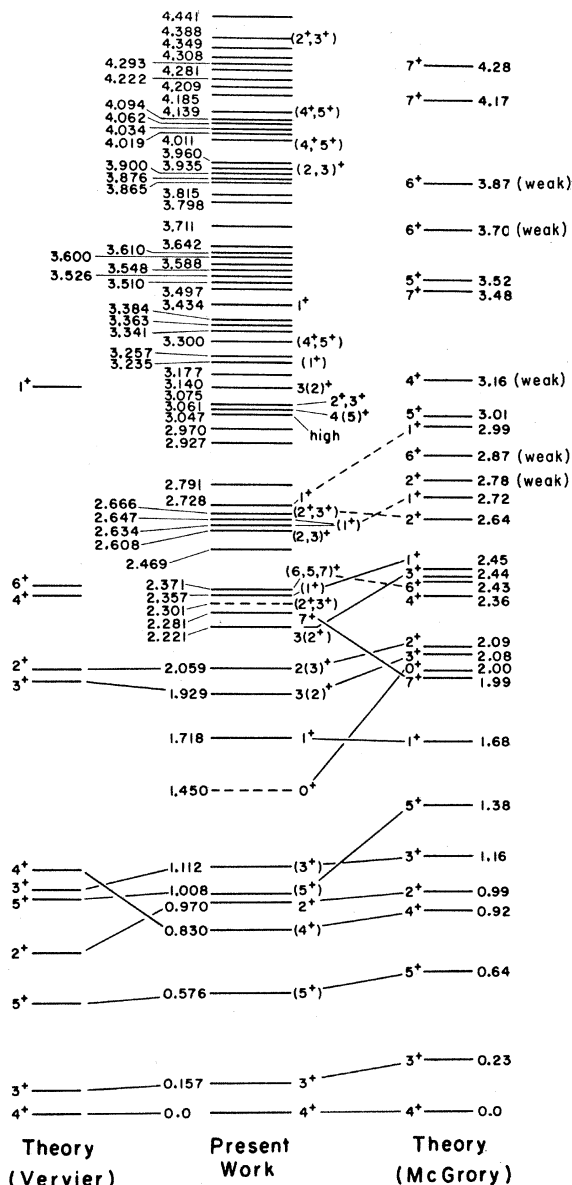


FIG. 7. Graphical comparison of results of present experiment with predictions of Vervier (Ref. 2) and McGrory (Ref. 3). For locations and  $J^\pi$  of low-lying  $\text{Co}^{56}$  levels, McGrory's levels marked "weak" are predicted to be excited in  $(d, \alpha)$  with cross section less than  $1 \mu\text{b}/\text{sr}$ . Dashed lines indicate tentative correlation of predicted and actual levels.

ther and allow two holes as well as one hole in the  $f_{7/2}$  shell in  $\text{Co}^{56}$ . Level locations and explicit deuteron pickup strengths for each configuration contributing to each of 28  $\text{Co}^{56}$  levels are predicted.

Figure 7 graphically compares Vervier's and McGrory's predictions with our experimental conclusions about the  $\text{Co}^{56}$  level scheme. It is seen that both approaches are successful in predicting the seven levels below 1.4 MeV, although McGrory's result is more significant, since Vervier used the energies of the lowest  $2^+$ ,  $3^+$ ,  $4^+$ , and  $5^+$  states to calculate his matrix elements to begin with. McGrory predicts the energy of the lowest  $1^+$  state almost perfectly, while Vervier's  $1^+$  state falls 1.4 MeV high of the mark, most likely due to neglect of its two-particle-two-hole components. All 18 levels predicted by McGrory below 2.75 MeV can be correlated, at least tentatively, with levels seen experimentally. Further correlation of McGrory's predictions and experimental states may be possible, but is hindered by the high level density above 2.4 MeV. The relative success of these two approaches tells us that the inclusion of two-particle-two-hole configurations materially improves predictions of the one-particle-one-hole scheme. Figure 8 shows McGrory's predicted and actual cross sections for calculated and observed states. There is reasonable quantitative agreement, with only one discrepancy larger than a factor of 3. Considering that predicted and ob-

served strengths vary over a factor of  $\sim 100$  the general agreement indicates a fair degree of success of the structure calculations of McGrory. A yet unanswered question is whether an even larger shell-model space would significantly increase agreement of theory and experiment for low-lying states, or whether a better reaction theory is needed at this point.

For  $\text{Pb}^{208}(d, \alpha)\text{Tl}^{206}$  Kuo's wave functions explained the experimentally observed enhancement of the lowest states of each  $J^\pi$ .<sup>21</sup> Bertsch,<sup>51</sup> on the other hand, predicted inhibition of  $(d, \alpha)$  to low-lying states of  $T=1$  nuclei. We have searched our results for agreement with either pattern and have found that the lowest identified  $5^+$  and  $7^+$  levels are each the strongest states of their spin, but the third  $3^+$  level is the strongest of the  $3^+$  states and the second  $2^+$  and  $1^+$  are stronger than the first of each spin. McGrory's specific wave functions predict correctly that only the lowest  $5^+$  and  $7^+$  transitions should be the strongest of their spin for  $\text{Ni}^{58}(d, \alpha)$ . Our results are in agreement with respect to low-level enhancement or inhibition, and suggest that structure details in  $\text{Co}^{56}$  tend to invalidate broader generalizations.

The direct  $(d, \alpha)$  reaction study has enabled us to give many new  $J^\pi$  and configuration assignments or suggestions for  $\text{Co}^{56}$ , and has largely verified many of McGrory's predictions about level locations and strengths. We have seen substantial evidence for  $p_{3/2}$  proton strength in the  $\text{Ni}^{58}$  ground state, extensive configuration mixing in  $\text{Co}^{56}$ , and numerous indications that many  $\text{Co}^{56}$  states below 2 MeV have nonnegligible two-particle-two-hole strength. The latter would explain the relatively much stronger excitation of the even  $J$  states in  $(p, \text{He}^3)$  compared to  $(d, \alpha)$ , the strong excitation of the ground state (relative to nearby levels) in  $(\text{He}^3, t)$ , the  $0^+$  level at 1.450 MeV, the slowness of  $\text{Ni}^{58} \beta^+$  decay to the 1.718-MeV level, the disagreement of this level's location with the  $\pi^{-1}\nu^{+1}$  calculation, and the over-all success of McGrory's predictions.

DWBA calculations using matching real wells to generate the form factor, and incoming and outgoing waves gave sizable improvements over those using conventional methods. Although there is some theoretical justification for this procedure, its usefulness over a wide range of nuclei is yet to be experimentally demonstrated. Our unusual value of the  $(d, \alpha)$  normalization constant  $N(d, \alpha)$  shows, at the very least, that there are many ambiguities to be removed before a universally useful value of  $N$  can be ascertained. We have presented some evidence for a  $J$  dependence in our  $L=4$  and perhaps  $L=2$  angular distributions, but this subject, too, needs further study.

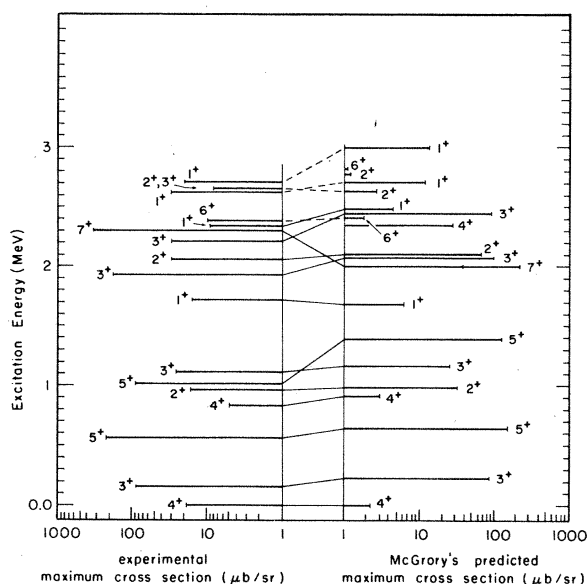


FIG. 8. Comparison of levels and excitation strengths predicted by McGrory with experimental values for those levels below 3 MeV. Other levels are not shown. Agreement is generally good, but there are some exceptions.

## VI. ACKNOWLEDGMENTS

We are grateful to Dr. J. B. McGrory for his kindness in making available  $\text{Ni}^{58}(d, \alpha)\text{Co}^{56}$  spectroscopic amplitudes, and to Dr. R. M. Drisko for

helpful discussions. The data-taking and programming assistance of R. DelVecchio, R. Gibson, and J. Childs are gratefully acknowledged. M. S. thanks the Westinghouse Electric Corporation for partial financial support.

\*Work supported by the National Science Foundation.

†Present address: Brookhaven National Laboratory, Upton, New York 11973.

<sup>1</sup>D. O. Wells, Nucl. Phys. **66**, 562 (1965).

<sup>2</sup>J. Vervier, Nucl. Phys. **78**, 497 (1966).

<sup>3</sup>J. McGrory, private communication.

<sup>4</sup>J. M. Laget and J. Gastebois, Nucl. Phys. **A122**, 431 (1968).

<sup>5</sup>P. Goode and L. Zamick, Phys. Rev. Letters **22**, 958 (1969).

<sup>6</sup>D. O. Wells, S. L. Blatt, and W. E. Meyerhof, Phys. Rev. **130**, 1961 (1963).

<sup>7</sup>R. C. Jenkins and W. E. Meyerhof, Nucl. Phys. **58**, 417 (1964).

<sup>8</sup>H. Ohnuma, Y. Hashimoto, and I. Tomita, Nucl. Phys. **66**, 337 (1965).

<sup>9</sup>C. J. Piluso, D. O. Wells, and D. K. McDaniels, Nucl. Phys. **77**, 193 (1966).

<sup>10</sup>T. A. Belote, W. E. Dorenbusch, and J. Rapaport, Nucl. Phys. **A109**, 666 (1968).

<sup>11</sup>C. Shin, B. Povh, K. Schadewaldt, and J. P. Wurm, Phys. Rev. Letters **22**, 1124 (1969).

<sup>12</sup>J. H. Bjerregaard, P. F. Dahl, O. Hansen, and G. Sidenius, Nucl. Phys. **51**, 641 (1964).

<sup>13</sup>S. A. Hjorth, Arkiv Fysik **33**, 147 (1966).

<sup>14</sup>P. G. Roos and C. D. Goodman, in *Proceedings of the Second Conference on Nuclear Isospin, Asilomar-Pacific Grove, California, 13-15 March 1969*, edited by J. D. Anderson, S. W. Bloom, J. Cerny, and W. W. True (Academic, New York, 1969), p. 297; C. D. Goodman, private communication.

<sup>15</sup>G. Bruge, A. Chaumeaux, H. D. Long, P. Roussel, and L. Valentin, Bull. Am. Phys. Soc. **14**, 1208 (1969).

<sup>16</sup>T. G. Dzubay, R. Sherr, F. D. Becchetti, Jr., and D. Dehnard, Nucl. Phys. **A142**, 488 (1970).

<sup>17</sup>G. Bruge and R. F. Leonard, Phys. Rev. C **2**, 2200 (1970).

<sup>18</sup>J. Richert, J. Phys. (Paris) **30**, 609 (1969).

<sup>19</sup>W. W. Daehnick and Y. S. Park, Phys. Rev. **180**, 1062 (1969); Y. S. Park and W. W. Daehnick, *ibid.* **180**, 1082 (1969).

<sup>20</sup>M. B. Lewis, Phys. Rev. C **1**, 501 (1970).

<sup>21</sup>M. B. Lewis and W. W. Daehnick, Phys. Rev. C **1**, 1577 (1970).

<sup>22</sup>J. E. Spencer and H. A. Enge, Nucl. Instr. Methods **49**, 181 (1967).

<sup>23</sup>G. R. Satchler, Nucl. Phys. **55**, 1 (1964); R. H. Bassel, R. M. Drisko, and G. R. Satchler, Oak Ridge National Laboratory Report No. ORNL-3240, 1962 (unpublished).

<sup>24</sup>N. K. Glendenning, Ann. Rev. Nucl. Sci. **13**, 191 (1963); N. K. Glendenning, Phys. Rev. **137**, B102 (1965).

<sup>25</sup>G. Mairle and U. Schmidt-Rohr, Max Planck Institut für Kernphysik (Heidelberg) Report No. 1965 IV 113 (unpublished).

<sup>26</sup>W. W. Daehnick, Phys. Rev. **177**, 1763 (1969).

<sup>27</sup>B. L. Cohen, Rev. Sci. Instr. **33**, 85 (1962).

<sup>28</sup>J. Childs, unpublished.

<sup>29</sup>R. Schoneberg and A. Flammersfeld, Z. Physik **200**, 205 (1967); R. Beraud *et al.*, Nucl. Phys. **A99**, 577 (1967); H. H. Bolotin and H. J. Fischbeck, Phys. Rev. **158**, 1069 (1967).

<sup>30</sup>S. Raman, Nucl. Data Sheets **B2**(No.5), 43 (1968), and references cited therein.

<sup>31</sup>B. F. Bayman and N. M. Hintz, Phys. Rev. **172**, 1113 (1968), and references cited therein.

<sup>32</sup>J. J. Kolata, L. S. August, and P. Shapiro, Phys. Rev. C **3**, 296 (1971).

<sup>33</sup>T. A. Brody and M. Moshinsky, *Tables of Transformation Brackets for Nuclear Shell-Model Calculations* (Direccion General de Publicaciones, Universidad Nacional de Mexico, Ciudad Universitaria, Mexico, D. F., 1960).

<sup>34</sup>P. D. Kunz, University of Colorado Report, 1967 (unpublished).

<sup>35</sup>R. M. Drisko and F. Rybicki, Phys. Rev. Letters **16**, 275 (1966); and private communication. We are grateful to the authors for making code MIFF available to us.

<sup>36</sup>F. D. Becchetti, Jr., and G. W. Greenlees, Phys. Rev. **182**, 1190 (1969).

<sup>37</sup>I. Talmi, Helv. Phys. Acta **25**, 185 (1952).

<sup>38</sup>M. J. Schneider, Ph.D. thesis, University of Pittsburgh, 1971 (unpublished).

<sup>39</sup>C. M. Perey and F. G. Perey, Phys. Rev. **132**, 755 (1963).

<sup>40</sup>L. McFadden and G. R. Satchler, Nucl. Phys. **84**, 177 (1966).

<sup>41</sup>R. Bock *et al.*, Nucl. Phys. **A92**, 539 (1967).

<sup>42</sup>E. M. Henley and D. V. L. Yu, Phys. Rev. **133**, B1445 (1964).

<sup>43</sup>R. DelVecchio and W. W. Daehnick, to be published; R. DelVecchio, W. W. Daehnick, D. L. Dittmer, and Y. S. Park, Phys. Rev. C **5**, 1989 (1971).

<sup>44</sup>R. Stock, R. Bock, P. David, H. H. Duhm, and T. Tamura, Nucl. Phys. **A104**, 136 (1967).

<sup>45</sup>M. H. Macfarlane, in *Proceedings of the International Conference on Properties of Nuclear States, Montreal, Canada, 1969*, edited by M. Harvey *et al.* (Presses de l'Université de Montréal, Montréal, Canada, 1969), p. 385.

<sup>46</sup>R. J. Ascutto and N. K. Glendenning, Phys. Rev. C **2**, 1260 (1970).

<sup>47</sup>W. Dobrowski, R. V. Jones, and C. D. Jeffries, Phys. Rev. **101**, 1001 (1956); R. V. Jones, W. Dobrowski, and C. D. Jeffries, *ibid.* **102**, 738 (1956).

<sup>48</sup>M. J. Schneider and W. W. Daehnick, Bull. Am. Phys. Soc. **15**, 62 (1970).

<sup>49</sup>R. A. Hinrichs, R. Sherr, G. M. Crawley, and I. Proctor, Phys. Rev. Letters **25**, 829 (1970).

<sup>50</sup>C. C. Lu *et al.*, Phys. Rev. **186**, 1086 (1969).

<sup>51</sup>G. Bertsch, Phys. Letters **25B**, 62 (1967).